Characterization of Human Liver Stromal Cells

Citation

Permanent link

Terms of Use

Share Your Story

Characterization of Human Liver Stromal Cells

Samantha Guinn

A Thesis Submitted to the Faculty of

The Harvard Medical School

in Partial Fulfillment of the Requirements

for the Degree of Master of Medical Sciences in Immunology

Harvard University

Boston, Massachusetts.

May, 2017

Thesis Advisor: Dr. Arlene Sharpe   Samantha Guinn

Characterization of Human Liver Stromal Cell Markers

The liver is a highly immunologic, metabolic organ in the body with many functions including but not limited to amino acid and carbohydrate metabolism, synthesis of plasma proteins, metabolism of pharmaceuticals, defense against pathogens, and more. There are two types of stromal cells in the liver: liver sinusoidal endothelial cells and hepatic stellate cells. The goal of this thesis is to determine markers that can be used to identify human stromal cells. I investigated the expression of cellular surface and intracellular molecules on human stromal cells isolated from human livers. The cellular markers for this work in human samples were modeled after published data in mice. In order to test the stability of the expression of these markers *in vitro*, multiple stromal cell lines were generated from the human stromal cells, and different passage numbers of each cell line tested using flow cytometry. Phenotypic and morphological changes were found across multiple passage numbers where the stromal cells start to lose their strict structure. In addition to morphological changes, changes in expression of cellular markers were also identified. VCAM-1 (CD106) is changed across different passages and also reproduced across numerous cell lines. Cellular adhesion marker CD146 expression is also altered, and when coupled with antigen uptake of Ova via scavenger receptors on LSECs there is a strong shift in populations from single positive for each marker, scavenger receptor and CD146, to double positive across subsequent passages. Our identification of stromal cell markers can be used for further experiments for cellular sorting and functional studies of stromal cells.

Table of Contents

Figures
Figure 1.1: The Hepatic Sinusoid. The hepatic sinusoid is set up in a way that allows for all cell types to have interaction with the environment. The LSECs form a continuous lining of the liver sinusoids which separates the parenchymal, or fat storing cells, being the hepatic stellate cells. The LSECs lack a basement membrane and have open pores which help constitute the structure of the wall of the hepatic sinusoid. By allowing blood to pass from the sinusoid to the parenchyma, antigen uptake may occur. Kupffer cells also have direct access as the primary phagocytic cells in the environment. Dendritic cells are the sentinel cells surveying the microenvironment for pathogen. Hepatic Stellate Cells are known to live in the Space of Disse in between the hepatocytes and the endothelium which supports the LSECs having primary interaction with the blood and then the HSCs having secondary interaction. HSCs are also key players in regulation of blood flow due to their location and the size of the cells. (Figure is modified from Thomson and Knolle, Nature Reviews Immunology).

Figure 3.1: Growth rates between livers.
(A) Growth rate between P0 and P1: This figure demonstrates the amount of time it took each sample to become confluent enough in the T25 Falcon flask to be split into a T75 Falcon flask **(B).** Growth rate between P1 and P2. After confluence was achieved in the T75 Falcon flask, the cells were split into a T175 Falcon flask as passage 2 **(C).** Growth from passage 2 to passage 3. The cells were split 1:2 from one T175 Falcon flask into two T175 Falcon flasks; average 5 days **(D).** Time between passages. Average time (days) from P0 to P1 is 19.43 days. Average time from P1 to P2 average is 5 days. Average time from P2 to P3 is 5.31 days **(D).**

Figure 3.2: Over subsequent passages the stromal cells showed morphological changes. Images represent sequential passages for the stromal cells. Passage 1 has more cells growing close together (A). Passage 2 has cells that look very similar to passage 1; they look healthy and proliferate well (B).

Obvious cell morphology changes are seen in passage 8 (C). Cells lost structure and proliferative ability; this only worsens throughout the subsequent passages. Passage 14 has cells that have lost structure (D).

Figure 3.3 Histograms showing positive and negative markers on Liver Sinusoidal Endothelial Cells. Representative histograms of positive markers include CD146 (**A),** scavenger receptor (OVA uptake (**B**), CD31 (**C**), CD54 (**D**), MHC I (**G**), MHC II (**H**), CD80 (**I**), and CD106 (**K**). Negative results, or very lowly expressed markers include CD32 (**E**), CD50 (**F**), CD86 (**J**), and CD206 (**L**). Each panel includes unstained, isotype control, passage 5 (red), passage 7 (cyan), and passage 9 (green) except from OVA (B). Isotype control not applicable for OVA uptake.

Figure 3.4 Mean Fluorescence Intensity (MFI) of markers on Liver Sinusoidal Endothelial Cells. The statistical data from figure 3.3 are represented and quantified here. Each marker and its respective MFI was quantified to show which marker is expressed and to what degree. All markers were tested with an isotype control (grey). Each bar graph includes unstained, isotype control, passage 5 (red), passage 7 (cyan), and passage 9 (green) except from OVA (B. Isotype control not applicable for OVA uptake; unstained included for OVA.

Figure 3.5 Hepatic Stellate Cells marker identification can be seen across different passage numbers. Representative histograms of the markers that were investigated for hepatic stellate cells. CD14 is seen as a positive marker (A) as is Vimentin (B) and only one sample for ⍰-SMA (C, far right). Podoplanin (G) also has high levels of positive expression. Negative expression can be seen in GFAP (D) and three of four samples in CD38 (E).

Figure 3.6 Mean Fluorescence Intensity (MFI) of Hepatic Stellate Cells. Statistical data of figure 3.5 are shown with the MFI data. MFI is quantified to show which marker is expressed and

to what degree. All markers were tested with an unstained control and an isotype control (grey). Each bar graph includes isotype control, passage 5 (red), passage 7 (cyan), and passage 9 (green). Positive expression is seen in HSC activation marker CD14 (A), intracellular stain for Vimentin (B), and podoplanin (F). Negative expression is seen in CD38 (D), very low expression is seen in Desmin (E).

Figure 3.7 Population shift in CD146+ OVA+ cells across passages. Representation of contour plots show dramatic shifts in cellular populations for CD146+ OVA+ cells across different passages that include passage 5, passage 7, and passage 9 for human liver sample digested on 8/17/16 (**A, left to right).** The cellular population shift between a low population of CD146+ OVA+ for passage 5 increases in different samples as well, this can be represented in human liver sample 12-21-16 (**B, left to right).** The shift in population can be seen in samples that have either not undergone chemotherapy treatment and those that have (**A and B).**

Figure 3.8: In order to fully understand how the population has shifted, MFI from figure 3.7 was calculated for each sample, for OVA, CD146 and CD146 expression compared to Isotype (**A and B).** 8/17/16 (**A**). 12/21/16 (**B**). While the OVA population didn't increase as dramatically as expected (**A and B left),** CD146 MFI increased drastically across passage numbers (**A and B, right).** The total number of cells that presented with this double positive population increased across passage numbers and is shown as a frequency of total bar graph (**C).**

Tables

Table 1.1: Table 1.1 List of Liver Sinusoidal Endothelial Cell Surface Markers that were tested. Table indicates markers previously tested in mice. All cell markers listed are surface markers.

Table 1.2: List of Hepatic Stellate Cell markers; Surface and Intracellular. *intracellular markers

Table 1.3 (Appendix): Human tissue sample data and observation allow for characterization of disease and origin of sample. The quantification of data that is acquired from these samples informs experimental design based on selection of patient populations; i.e. male vs female experiments, similar diagnosis, chemotherapy treatment and other options. *patient underwent chemotherapy **patient underwent radiation treatment

Acknowledgements

I would like to say a huge and gracious thank you to Frank Schildberg for his mentorship over the course of the year, I wouldn't have been able to accomplish this without him. His guidance has been instrumental in my educational career. My experience would have been very different had I not had the support from Frank and the entire Sharpe Lab. I also would like to send a thank you to Mike Peluso for his guidance and teaching as well. Working with Mike has been invaluable. Lastly, a large thank you to Dr. Arlene Sharpe for providing me this incredible opportunity to work in her lab as a Masters student.

Thank you to the MMSc Immunology program at HMS; Shiv Pillai and Mike Carroll for their involvement and guidance in my education and for their constant mentorship. Also, thank you to Selina Sarmiento and Megan Eruzione.

"This work was conducted with support from Students in the Master of Medical Sciences in Immunology program of Harvard Medical School. The content is solely the responsibility of the authors and does not necessarily represent the official views of Harvard University and its affiliated academic health care centers."
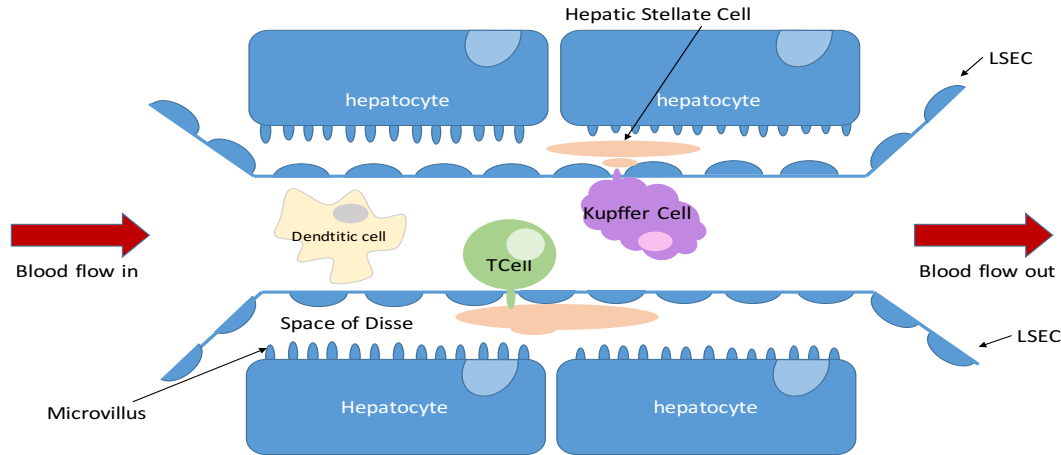
Chapter 1: Background

1.1 Introduction:

The liver is a highly immunologic organ with the power to possess many different functions that may impact the whole body. The liver is the body's largest internal organ that is responsible for glycogen synthesis, bile production, processing food, amino acid and carbohydrate metabolism, synthesis of plasma proteins, metabolism of pharmaceuticals, defense against pathogens, oral tolerance, and other functions. With all of these abilities it is no wonder that this organ is vital to maintenance of life and why many of the interactions that take place in the liver are translatable. The liver sits just above the stomach in the body cavity and allows for an ease of access of food antigens to be recognized via gut transport and thus oral tolerance. The identification of oral tolerance in the body is highly important because it allows for a nonresponse to innocuous food antigens. This will facilitate digestion rather than provoking an immune response when the body does not need to have one.

The liver is such a vital organ that, when damaged by disease, the consequences can be detrimental to the body. There is interest in the use of liver stromal cells for therapy. A number of studies have investigated how stromal cells impact diseases including but not limited to hepatitis, cirrhosis, cancers, medicinal damage, fibrosis, inflammatory liver diseases, and others. This is incredibly important work since over one million Americans alone are infected with Hepatitis B, over four million Americans are infected with Hepatitis C, 21,000 Americans are diagnosed every year with liver cancer, and on average 20% of Americans have fatty livers (American Liver Foundation, 2013). These diseases can cause cirrhosis and ultimately liver failure if not recognized and treated. Liver disease is on the rise as the fourth leading cause of death in the United States alone. Importantly, liver disease is increasing in children; over six million, have been diagnosed

with non-alcoholic fatty liver disease. While these statistics are incredibly alarming, hopefully with the understanding of how stromal cells interact in the liver with neighboring cells; resident and infiltrating, and how progression of disease occurs, there can advances in diagnosis and treatment of liver disease.

Stromal cells may actually be used therapeutically if able to be controlled. While stromal cells have positive features such as forming connective tissue, stromal cells also can have very negative effects when they are uncontrolled and can lead to fibrosis because of the excessive amount of collagen that is produced from stellate cells under liver injury. The excessive amount of collagen leads to scar tissue and ultimately cirrhosis and liver failure.

While liver stromal cells perform important work that impacts the entire organ, they only are a small percentage of cells in the organ. General make up of the liver is approximately 80% hepatocytes and the other 20% comprises a mixture of many other key players such as Kupffer cells, Liver Sinusoidal Endothelial Cells (LSEC), Hepatic Stellate Cells (HSC), T cells, Macrophages, and Antigen Presenting Cells such as Dendritic Cells. **Figure 1.1** represents a microscopic depiction of the hepatic sinusoid which has both of the stromal cell subsets identified as well as the other cells that make up the liver such as Kupffer cells, T cells and Dendritic cells. These cells live in the sinusoid where the smaller, flat HSCs are found in the space of Disse. In addition to the HSCs being resident in the space of Disse, the microvilli of the hepatocytes extend out and uptake proteins here which are seen in **Figure 1.1** which illustrates the complexity of the sinusoid and how each cell performs specific duties to maintain proper function. The make up of the liver sinusoid is complex but the identification of each cell type allows for further investigation into the cell-cell interactions in the organ and what role each cell plays.

Figure 1.1: The Hepatic Sinusoid. The hepatic sinusoid is set up in a way that allows for all cell types to have interaction with the environment. The LSECs form a continuous lining of the liver sinusoids which separates the parenchymal, or fat storing cells, being the hepatic stellate cells. The LSECs lack a basement membrane and have open pores which help constitute the structure of the wall of the hepatic sinusoid. By allowing blood to pass from the sinusoid to the parenchyma, antigen uptake may occur. Kupffer cells also have direct access as the primary phagocytic cells in the environment. Dendritic cells are the sentinel cells surveying the microenvironment for pathogen. Hepatic Stellate Cells are known to live in the Space of Disse in between the hepatocytes and the endothelium which supports the LSECs having primary interaction with the blood and then the HSCs having secondary interaction. HSCs are also key players in regulation of blood flow due to their location and the size of the cells. (Figure is modified from Thomson and Knolle, Nature Reviews Immunology).

The cellular subset of primary investigation in this project are the liver stromal cells. By definition stromal cells are and comprise the connective tissue of any organ including the lymph node, kidney, liver, and so on. Beyond being a connective tissue source in the body, stromal cells also support the function of many other cells in the body such as mesenchymal and parenchymal cells. Parenchymal cells, such as hepatocytes, are functional cells and mesenchymal cells are structural cells. Mesenchymal cells differentiate into many different structural cells such as stromal cells, osteoblasts, chondrocytes, and stromal cells. Studying stromal cells has led to understanding of their importance as a cellular subset and how differentiation may treat disease including cancers and cardiovascular disease by bone marrow derived mesenchymal stromal cells (BMDC) (Copland, 2011). BMDCs are especially useful in treatment of Sickle Cell Disease in that BMDCs are thought to help prevent Graft Versus Host Disease after transplantation because of the immunoregulatory properties that BMDCs possess; such as upregulation of MHC II under

inflammatory conditions which may help to stop rejection of transplants (Stenger, 2017). These examples demonstrate the necessity for stromal cells and their function. Beyond being a mediator in disease, stromal cells are also very versatile and have many capabilities across the body such as the creation of bone, cartilage, lymph nodes, and liver. There are many different types of stromal cells in the body, however HSC and LSEC are the two subsets in the liver. These two subsets have very different purposes in the liver including but not limited to; LSEC's having the ability to be immune surveyors and when activated HSC can produce collagen. When collagen production is not moderated, fibrosis and cirrhosis occur. The maintenance of cellular homeostasis is key in the liver and HSCs and LSECs are important regulators of liver homeostasis.

1.2 Liver sinusoidal endothelial cells

Liver Sinusoidal Endothelial Cells (LSEC) have a controversial history. Many individuals in the field didn't distinguish these cells as a distinct cell type until approximately 1978 when Eddie Wisse became the leading LSEC investigator. LSECs as a cell type have very unique properties such as possessing large amounts of endocytic vesicles. These vesicles and endocytic ability show the dynamics of LSECs and how they are so vitally important in antigen uptake via scavenger receptors on the cellular surface which surveys blood passing into the parenchyma through the sinusoids in the liver (Friedman, 2008). Although they possess the ability to perform antigen uptake, LSECs do not typically take up very large particles; that is reserved for the role of the Kupffer cells. A major difference between these two cell types is that LSECs aren't typically the phagocytic cells, the Kupffer cells are (Kawai, 2001). When the ability of the Kupffer cells is compromised, then the LSECs take on the role of being the phagocytic cell type which enables them to uptake particles up to 1 μm in size. LSECs play a role in liver homeostasis via the scavenger receptor system, allowing the LSECs to clear foreign antigen from circulation

(Evlvevold et al., 2008, Schurich, 2009). In addition to antigen uptake, LSECs also have major roles in blood flow in the body and directing the drainage from the lymphatic in the space of Disse. This also aids in the ability to uptake antigen and perform other immune functions. Beyond being surveyors of the immune system, LSECs have powerful capabilities in controlling inflammatory immune responses because LSECs have the ability to induce regulatory T cells by secreting TGF☐ which stimulates and primes regulatory T cells (Schildberg, 2015). LSECs also have very powerful abilities to cross prime naïve CD8 T cells and act as surveyors of the environment for microbial infections (Knolle, 2016). The LSECs uptake circulating antigen and present said antigen to CD8 T cells via MHC class I ligand. This process shows the interaction these cells have with neighboring cells and how versatile the LSEC population can be. In addition, LSECs have capabilities to interact with activated T cells by virtue of the LSECtin ligand which binds to LAG-3 and CD44. LSECtin interaction with LAG-3 restores interferon gamma secretion in cases of melanoma (Xu, 2014) and LSECtin interaction with CD44 is an incredibly important function of LSECs because this gives the cells the ability to inhibit T cell activation, which will dampen immune responses and/or induce apoptosis. When this process is defective, autoimmunity in the liver develops. Therefore, LSECs are instrumental in maintenance and control of autoimmunity by activated T cells. Lastly, LSECs also have the ability to interact with resident antigen presenting cells in the liver. This collaborative effort between of LSECs and dendritic cells can suppress dendritic cell priming of naïve T cells (Schildberg, 2015). Thus LSECs are instrumental to maintaining liver homeostasis while serving as immune surveyors via the scavenger receptor system (Braet, 2002).

1.3 Hepatic Stellate Cells

Hepatic Stellate Cells (HSC) are a peri-sinusoidal cell type which resides in the space of Disse in the liver. The HSCs have a special anatomy in that they span the circumference of the liver sinusoids and thus help in the maintenance and control of blood flow through the sinusoid which is mediated by contraction and reduction of the sinusoid (Knolle, 2016). Beyond having structural differences from LSECs, the HSCs have a specialized storage mechanism for Vitamin A. These cells have vesicles, both extracellular and intracellular for vitamin A storage. These cells represent the main storage for vitamin A in the body. Balance and storage of Vitamin A s important to the maintenance of teeth, soft tissue, skeletal tissue, mucus membranes and skin. When HSCs undergo activation, they lose the quiescent vitamin A storage and are pushed into an activated state which causes their proliferation. When HSCs become activated, they produce collagen; when this is produced in excess it can lead to cirrhosis. In addition to excessive collagen production, HSCs can become suppressive during fibrosis, which occurs from a secretion of inhibitory cytokines such as IL-10 and TGF□ after the HSCs have become activated (Schildberg, 2015). The activation of HSCs may be achieved by a number of different mechanisms such as loss of IL-10, activation by reactive oxygen species produced by Kupffer cells, inflammatory conditions (Rifaat, 2002). Therefore, the biological capabilities of HSCs are vastly different from LSECs in that HSCs have the ability to be a major benefit in the body with Vitamin A or a detriment, by producing excessive collagen potentially leading to cirrhosis.

1.4 Cellular Markers

Markers for mouse LSEC and HSC have been published. CD146 is expressed on endothelial cells, including LSECs and is important in supporting endothelial integrity (Schrange, 2008), as well as antigen uptake via scavenger receptors, demonstrated by OVA uptake (Limmer, 2000). CD45 is a marker used to exclude leukocytes and included to ensure specificity of the

subsets (LSEC and HSC) that were tested (**Table 1.1**). Other molecules expressed on LSECs include costimulatory molecules CD80 and CD86, MHC I and MHC II, as well as CD50 (ICAM-3) and CD54 (ICAM-1). CD106 (VCAM-1) expression on LSECs has been questionable. Activated hepatic stellate cells express CD14, □-SMA, Vimentin, and Desmin (**Table 1.2**). GFAP should be expressed in quiescent cells but GFAP expression is lost. CD38 is constitutively expressed in both *in vitro* and *in vivo* experiments of HSC (March, 2007). As stated previously, the markers that were tested for both cellular subsets; LSEC and HSC, were of those that had been previously characterized in mice which did include a finding of constitutive
 expression by express MHC I, MHC II, CD80 and CD86 (Schurich, 2009). We examined the expression of all of these molecules on human stromal cells (Table1.1, 1.2).

1.5 Human patients

Samples were acquired through a collaborative effort between Massachusetts General Hospital (MGH), the Ragon Institute, and Harvard Medical School. The samples were all deemed healthy tissue by the pathologists and doctors at MGH because the patients and samples resected didn't have a viral infection such as HIV, HCV, HPV or inflammatory liver diseases. The majority of patients presented with cancer of different forms including choloangiocarcinoma, colon cancer, metastatic renal cell carcinoma (**Appendix, Table 1.3**). The pathologists assured us the samples were taken at least 2 cm away from where the tumor presented in the liver. Size of samples varied as well as ease of digestibility of each sample (**Appendix, Table 1.3**). 7 out of 18 samples were from patients who had undergone chemotherapy treatment and one sample was from a patient who had radiation therapy, which adds another layer of complexity to the samples that were acquired.

Marker	LSEC	Function	Clone	Company
CD146	LSEC	Melanoma cell adhesion molecule (MCAM), marker for endothelial cell lineage	P1H12 (PE) (PerCP/Cy5.5)	Biolegend
CD31	LSEC	Platelet endothelial cell adhesion molecule (PECAM-1), removing aged neutrophils from body	WM59	Biolegend
CD45		Leukocyte exclusion	H130	Biolegend
CD106	LSEC	Vascular Cell Adhesion Molecule-1, Leukocyte-endothelial cell adhesion	429MVCAM.A	Biolegend
CD50	LSEC	Intracellular Adhesion molecule 3; signaling molecule	CBR-IC3/1	eBioscience
ALEXA-647 OVA	LSEC	Scavenger receptor uptake and presentation		ThermoFisher Scientific
LYVE-1	LSEC	Lymphatic Vessel Endothelial Receptor 1, transmembrane receptor for extracellular matrix glycosaminoglycan HA	OAAB21889	Aviva systems Biology
MHC I	LSEC	Bind peptide fragments from proteins and display them on the cellular surface for T cell recognition	TU36	Biolegend
MHC II	LSEC	Antigen presentation from exogenous sources primarily to CD4+ T cells	W6/32	Biolegend
CD80	LSEC	B7-1; costimulatory signal required for T cell activation	2D10	Biolegend
CD86	LSEC	B7-2; costimulatory signal required for T cell activation	BU63	ThermoFisher Scientific
CD32	LSEC	IgG Fc receptor; most abundantly distributed in human body, expressed on myeloid and lymphoid cells	FUN-2	Biolegend
CD206	LSEC	Mannose Receptor, C-type lectin	MMR 15-2	Biolegend
CD54	LSEC	Intracellular Adhesion Molecule – 1, signaling molecule		Biorbyt
ZOMBIE NIR		Live/Dead identification		ThermoFisher Sientific

Table 1.1 List of Surface Markers that were tested in Human Liver Sinusoidal Endothelial Cells. Table lists markers that were previously tested in mice. All cell markers listed are surface markers.

Marker	HSC	Function	Clone	Company
VIMENTIN *	HSC	Maintenance of cellular shape; major protein of mesenchymal cells	2D1	Antibodies online
CD14	HSC	Hepatic Stellate Cell activation marker	Monoclonal (HVimentin)	Biolegend
CD38	HSC	Cyclic ADP ribose hydrolase, present on surface of immune cells	HB-7	Biolegend
ALPHA-SMA*	HSC	Actin isoform, stellate cell activation	17H19L35	ThermoFisher Scientific
GFAP*	HSC	Stellate cell activation	REA335	miltenyibiotech
DESMIN*	HSC	Stellate cell identification	IgG1 Monoclonal [4G1]	Lifespan Biosciences, Inc.
PODOPLANIN	HSC	Mucin-type protein	NO-08	Biolegend
ZOMBIE NIR		Live/Dead identification		ThermoFisher Scientific

Table 1.2 List of Hepatic Stellate Cell markers; Surface and Intracellular. *intracellular markers

1.6 Questions Addressed in this Thesis

In this thesis, we sought to identify cellular markers, surface or intracellular, for human liver stromal cells (Hepatic Stellate Cells or Liver Sinusoidal Endothelial Cells). Characterization of stromal cells in human samples has been limited; this thesis hopefully will provide a better understanding of the markers that can be detected on human liver stromal cells. Markers defined on mouse liver stromal cells served as a useful benchmark for comparison and inspiration for our human project. We first examined markers expressed by mouse stromal cells in our experiments with human samples to determine what markers are present and to what degree. We also investigated how human stromal cells grow in culture and compared stromal cells at different passage numbers for expression of markers and their integrity. We have determined stromal cell growth patterns and identified some stromal cell markers for human Hepatic Stellate Cells and Liver Sinusoidal Endothelial Cells.

Chapter 2: Materials and Methods

Section 2:1: Tissue digestion. Human samples were obtained through a collaboration between The Ragon Institution, Harvard Medical School and the Massachusetts General Hospital surgical department. Each sample obtained from patients was qualified as healthy unless documented otherwise by hospital specialists. Documentation of treatment, therapy, medication and other variables in the samples were recorded for research purposes as well. Tissues obtained from patients with cancers have resections taken approximately 2 cm away from the tumor. Samples from patients that had undergone chemotherapy or radiation were documented and were digested using the same protocol as the other samples to create a standardized protocol. Samples were digested using a solution of 15mL PBS +/+ (Invitrogen), DNAse (Akron Biotech), and Collagenase (Worthington Biochemical) to form a digestion buffer kept at 37 °C. Samples were cut into as small of pieces as possible to allow for adequate digestion and placed into the digestion buffer for 20 minutes at 37 °C. This time was to allow for sufficient digestion of the sample. Samples were mixed once at 10 minutes. Samples were passed through a metal strainer in order to completely dissociate the tissue, separate out the cells from fat, and complete the digestion process. Next, cells were transferred into at 50 mL Falcon Conical tube and spun in the centrifuge at 1800 g for 5 minutes. Cells were then washed two times with phosphate buffered saline (PBS, Invitrogen) and spun at 1800 G for 5 minutes during each washing step. The supernatant was aspirated carefully from the conical after each spin while the pellet of cells remained at the bottom of the conical tube. The cells were then resuspended in 5 mL of the ALPHA MEM, + L-Glutamine, -Deoxyribo, -Ribonucleodite (Life Technologies), 30% fetal bovine serum (FBS) (Sigma), 1 % penicillin- streptomycin (100 U penicillin and 100 µg streptomycin (Invitrogen)), and plated into a T25 Falcon Flask and immediately placed in a 5% CO_2 incubator at 37 °C.

Section 2.2: Cell Culture: Each cell line was maintained for many passage numbers to help understand longevity of the cells and compare growth rates and stability of the cell lines across different passages. As each liver was from a different donor, each has a different profile of digestion aspects, growth rates, resiliency, longevity, and ability to withstand dissociation using 0.05% Trypsin (ThermoFisher Scientific). Cells were maintained using in ALPHA MEM, + L-Glutamine, -Deoxyribo, -Ribonucleodite (Life Technologies). To make the media complete, one bottle of 500 mL ALPHA MEM, + L-Glutamine, -Deoxyribo, -Ribonucleodite (Live Technologies) was used plus 30% FBS (Sigma) and 1% penicillin- streptomycin (Invitrogen), to be called ALPHA MEM complete. One of the most important aspects for cellular maintenance was not only changing the media immediately the next day following the digestion process, but was also changing the media a second day in a row for those cells in the T25 Falcon Flask. This step became important for removing the remaining fat cells and dead cells from the stromal cells to give optimal nutrients to the cells that were growing. When cells became confluent across the T25 at approximately 19 days, the cells were dissociated using 0.05% Trypsin (ThermoScientific). 10 mL of ALPHA MEM, + L-Glutamine, -Deoxyribo, -Ribonucleodite (Life Technologies), 30% FBS (Sigma), 1 % penicillin- streptomycin (100 U penicillin and 100 μg streptomycin (Invitrogen)), was added to neutralize the 0.05% Trypsin (ThermoFisher Scientific). Cells were spun at 1800 g for 5 minutes in the centrifuge. Supernatant was aspirated off and cells were resuspended in 15 mL of ALPHA MEM complete media and plated into a T75 Falcon Flask. When cells became confluent across the T75 at approximately 5 days, the cells were dissociated and washed as described above, and resuspended in 15 mL of ALPHA MEM, + L-Glutamine, -Deoxyribo, -Ribonucleodite (Life Technologies), 30% FBS (Sigma), 1 % penicillin- streptomycin (100 U penicillin and 100 μg streptomycin (Invitrogen)) media and plated into a T175 Falcon

Flask. Each flask was subsequently split at 1:2 in order to keep enough cells in the flask to allow for differentiation and proliferation. 1:3 proved too sparse for the cells to grow very well.

Section 2:3 Cell Freezing: Flasks with stromal cells used for freezing were first washed with PBS-/- (Invitrogen) to help with dead cell clearance and then trypsinized using 5 mL of trypsin (ThermoFisher Scientific) placed into the flask for approximately 1.5 minutes to allow for cells to be detached from the flask. 10 mL of ALPHA MEM, + L-Glutamine, -Deoxyribo, -Ribonucleodite (Life Technologies), 30% FBS (Sigma), 1% penicillin- streptomycin (Invitrogen) mixture was added to the flask to neutralize the trypsin (ThermoFisher Scientific). Cells were collected and transferred to a 50 mL conical and spun at 1800 G for 5 minutes to form a pellet. The Trypsin/media mixture was aspirated, and Cells were resuspended in the same media, Flasks that were frozen down in cryovials were frozen in a 2 cryovials to 1 flask ratio. Cells to be frozen were resuspended in a 500 µL per cryovials of the ALPHA MEM complete and 500 µL of the freezing media (8mL FBS (Sigma) + 2ML DMSO (Sigma)) per every ½ flask. Once the Freezing media (8mL FBS (Sigma) + 2ML DMSO (Sigma)) were added to the cryovials with the cell mixture, they were immediately placed on ice in a Mr. Frosty cooling chamber to be placed in the freezer. The chamber cools the cells at 1 °C per hour to not lose as many cells to freezing procedures. Mr. Frosty was placed in the -80 °C freezer for 24 hours and cells in cryovials were then transferred into liquid nitrogen for long term storage.

Section 2:4 Thawing of cells: Cryovials that were placed in the liquid nitrogen must be thawed with the utmost care due to the cytotoxic effect of DMSO (Sigma) on the cells. Vials were thawed using a water bath at 37 °C to bring them to room temperature quickly. Vials were thawed to approximately 75% and then the contents added to ALPHA MEM complete media that had been warmed to 37 °C. The DMSO (Sigma) mixture was replaced with the media mixture mentioned

above to keep as many cells as possible alive. Media in the flask was changed the next day in order to ensure that any remaining DMSO (Sigma) had been aspirated off and to provide for adequate nutrients.

Section 2.5: Flow Cytometry: Surface marker and intracellular staining of cellular markers was performed in the dark at 4°C.. MACS buffer (1% FBS (Sigma), PBS -/- (Invitrogen), 2mM EDTA (Invitrogen)) was used to maintain cells during the procedure. **Table 1.1** lists the antibodies, clone, and company from which they were purchased. Cells were plated in 96 well plates in order to have a more standardized procedure for use with the multichannel pipet. The multichannel pipet made the measurements more accurate and time required for staining shorter. Surface markers, Fc block, Live/Dead staining were all incubated for 20 minutes at 4°C. Surface markers were stained at a 1:200 dilution of antibody to MACS buffer at 4°C and Live/Dead stain was used at a 1:1000 dilution to MACS buffer. Intracellular staining was accomplished using the eBioscience intracellular staining kit after the completion of surface marker staining. 200 µL of IC Fixation Buffer (eBioscience) was added to each well and incubated on ice and protected from light for 30 minutes at 4°C. Cells were then spun for 2 minutes at 2280 g. 200 µL of 1X permeabilization buffer (eBioscience) was added to each well and spun for 5 minutes, supernatant was discarded and repeated. Cells were then resuspended in 100 µL of 1X permeabilization buffer (eBioscience). Intracellular antibodies were added to each well at a 1:200 concentration and incubated on ice, protected from light for 30 minutes. Cells were spun at 1900 RPM for 2 minutes, supernatant discarded. The cells were resuspended in 200 µL of the MACS buffer and spun at 1900 RPM for 2 minutes. Supernatant was discarded and cells were resuspended in 200 µL of permeabilization buffer to which the secondary antibody was added at a 1:200 concentration and incubated on ice with protection from light for 20 minutes at 4°C. Cells were spun at 1900 RPM for 2 minutes,

supernatant was discarded and cells were resuspended in 2000 µL of permeabilization buffer. Cells were spun at 1900 RPM for 2 minutes, supernatant was aspirated and discarded. Cells were resuspended in 200 µL of MACS buffer. Flow cytometry was performed using the LSR II instrument from BD Biosciences and data c analyzed using FlowJo v10.1 (FlowJo, LLC).

Section 2.6: Statistical Analysis. Statistical analysis was completed using Prism.

Chapter 3: Results

Section 3.1: Human samples vary as far as size, digestion process, and growth rate. Samples that were acquired for digestion ranged in size, color, appearance; some presented with white nodules, some had very red spots on them, certain samples had darker coloring, some had excessive amounts of fat, and each was different from the next. Some tissues sizes were much larger than others and some samples had much more fat remaining after the digestion process had been completed **(Appendix, Table 1.3).** Certain tissue samples were much tougher regarding digestion than others which could have been due to fibrosis or other factors. Although the patients presented with different backgrounds, the most common reason for resection was due to a choloangiocarcinoma diagnosis. All samples were negative for viruses including HIV, HPV, HCV. Most patients were female and ranged from 55 years of age to 82 years of age (**Appendix, Table 1.3).** Not only did the samples present very differently visually and differ in digestion, but the sample growth patterns varied greatly as well. Stromal cells grew very slowly from the initial digestion to confluence in the original T25 flask (**Figure 3.1**). The first passage occurred at day 19 on average and cell passaging became a much quicker process after the cells started to grow. Approximately 5 days after the original passage into a T75 flask the cells were then ready to be split into a T175 (**Figure 3.1**). This became an average benchmark for how often the cells needed to be passaged.
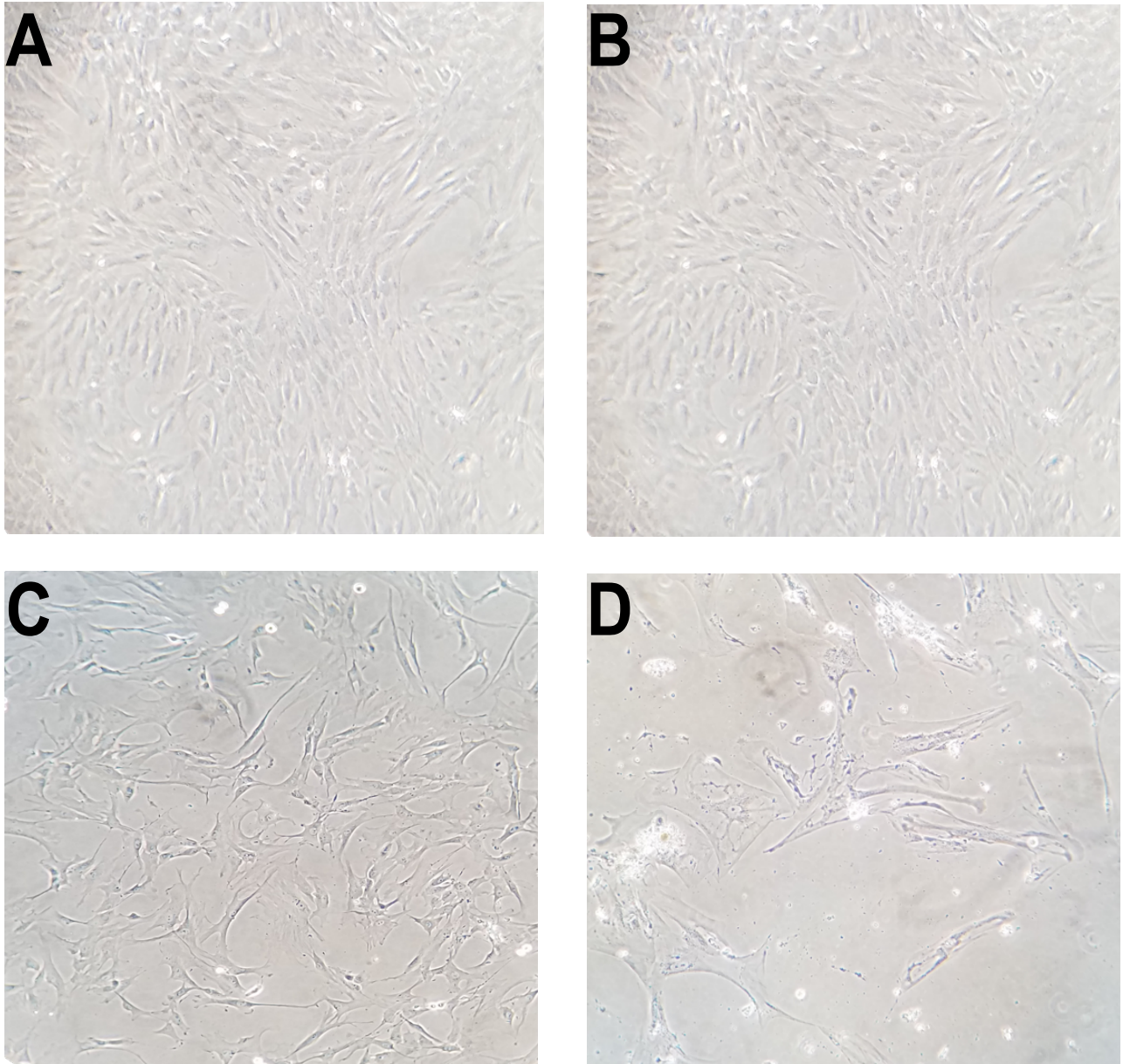
While the cells grew very well together, the morphology of the cells changed as the passage numbers got higher in that the cells became looser cells and didn't maintain structure While this is a very interesting finding, unfortunately, there was not a specific passage number where this occurred; it was different for every sample. Some samples started to lose their morphology at passage 8 and others lost their stringent morphology at passage 14 **(Figure 3.2).**
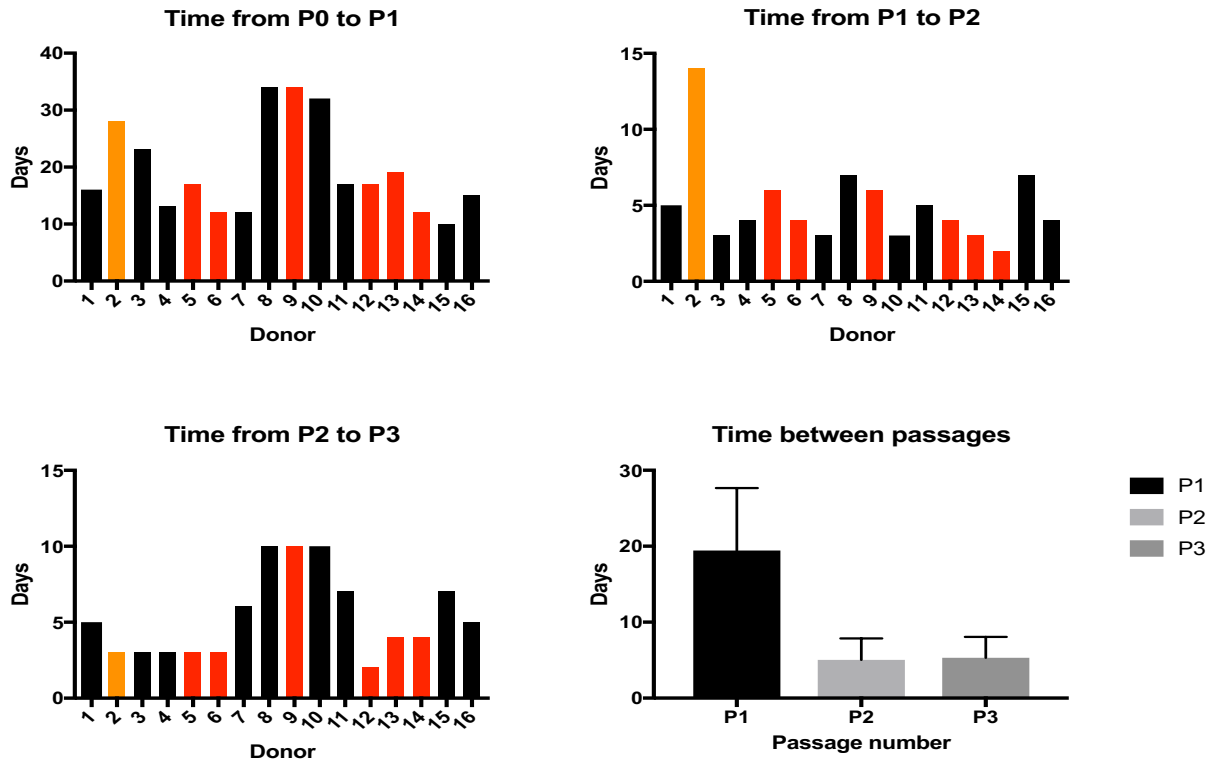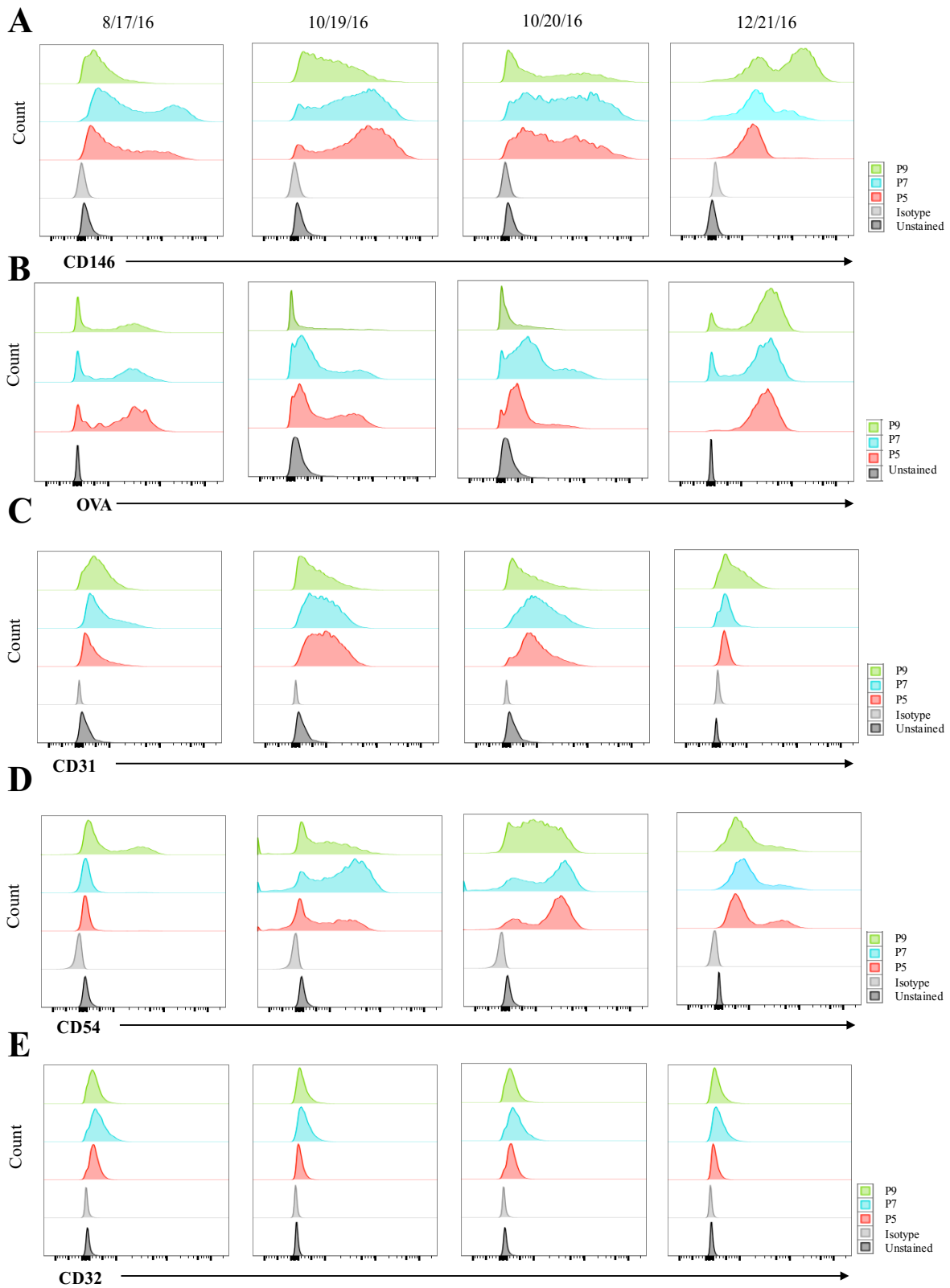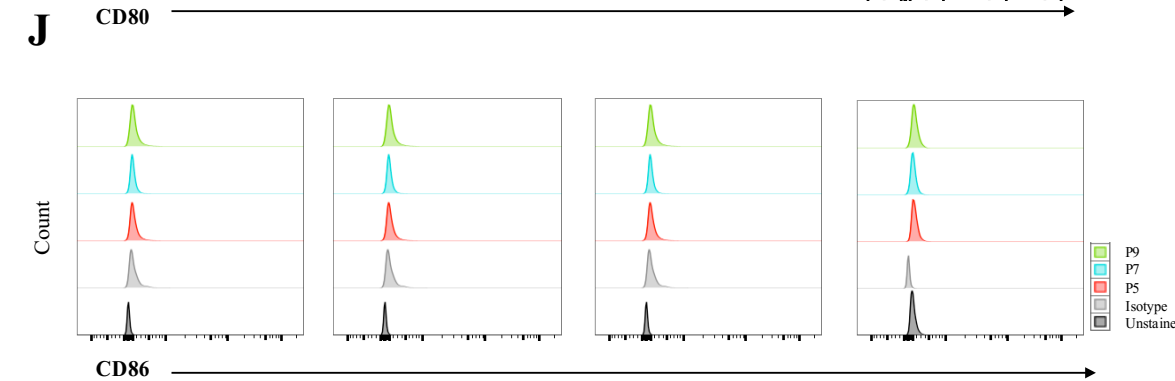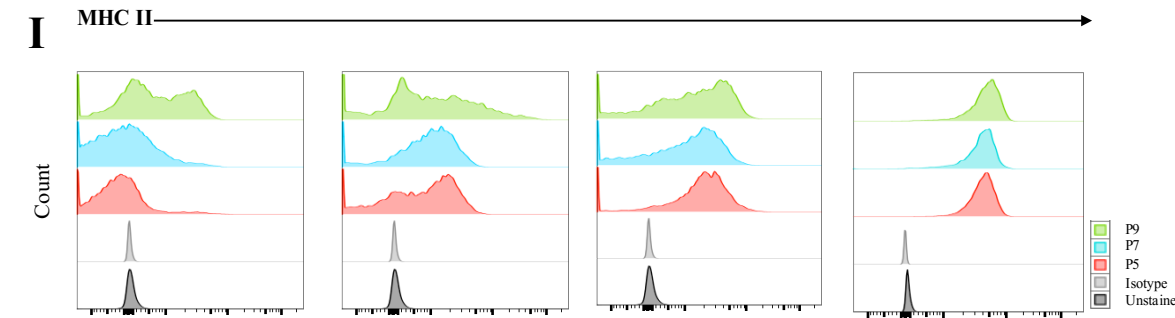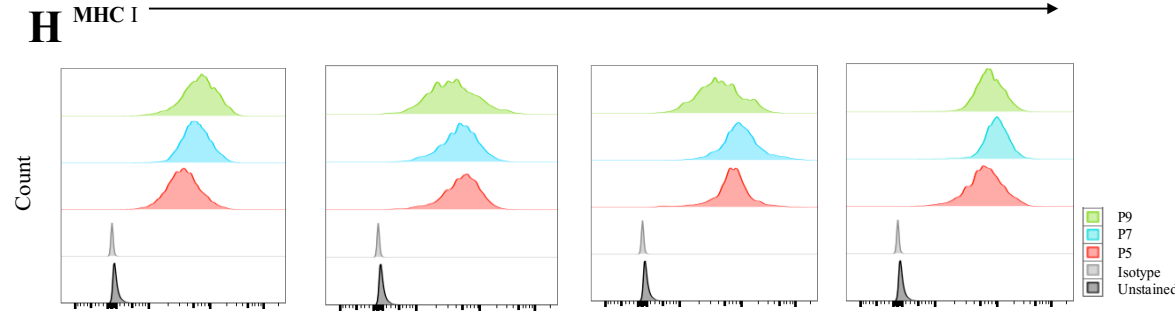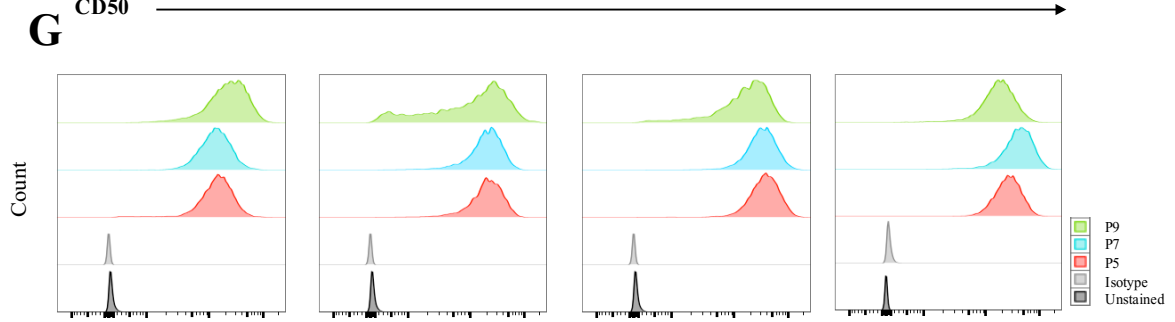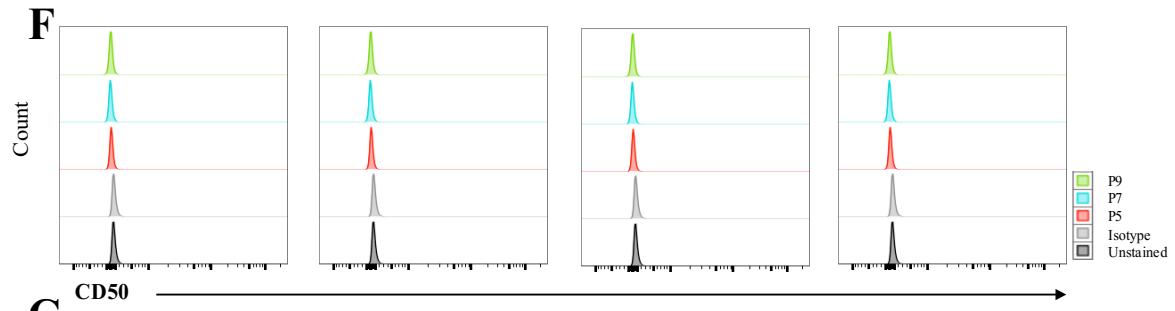
Figure 3.1: Growth rates between livers.

(A) Growth rate between P0 and P1: This figure demonstrates the amount of time it took each sample to become confluent enough in the T25 Falcon flask to be split into a T75 Falcon flask **(B).** Growth rate between P1 and P2. After confluence was achieved in the T75 Falcon flask, the cells were split into a T175 Falcon flask as passage 2 **(C).** Growth from passage 2 to passage 3. The cells were split 1:2 from one T175 Falcon flask into two T175 Falcon flasks; average 5 days **(D).** Time between passages. Average time (days) from P0 to P1 is 19.43 days. Average time from P1 to P2 average is 5 days. Average time from P2 to P3 is 5.31 days **(D).**
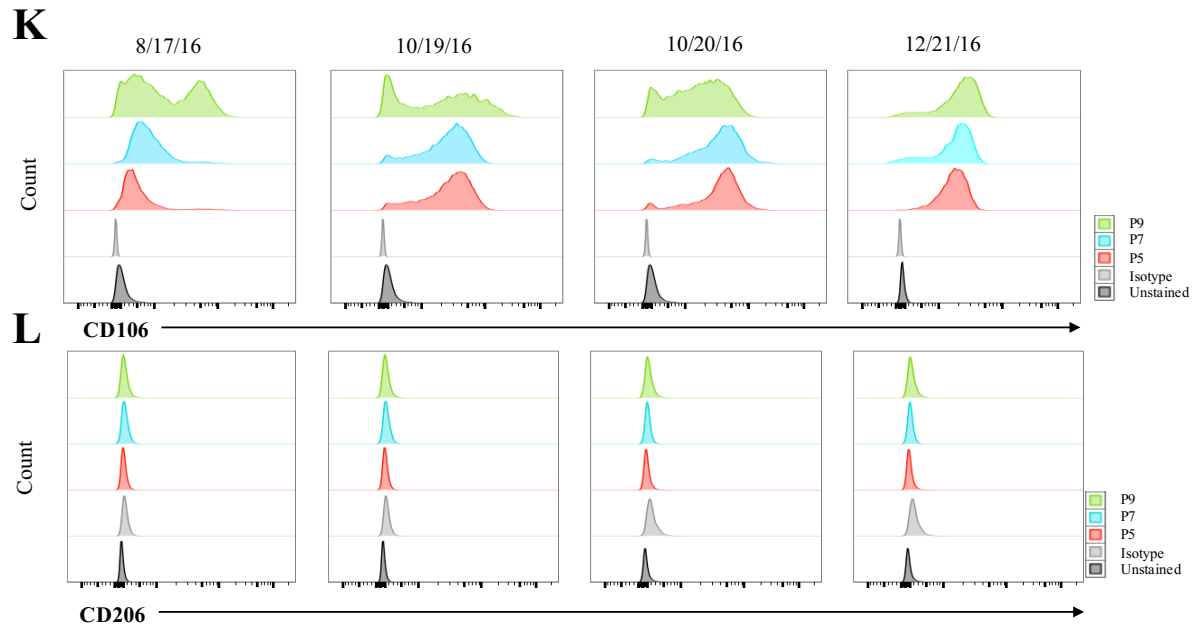
3.2 Identification of markers for Liver Sinusoidal Endothelial Cells. Based on previously published data identifying markers for LSEC in mice. we selected the markers to test on human samples (Friedman, Knolle, Schildberg). We explored CD146, CD31, scavenger receptor which is represented by OVA, mannose receptor, CD32, MHC I, MHC II, costimulatory receptors CD80 and CD86. In order to fully understand the stability of these markers, we compared their expression in cell lines over several passages. Passage numbers tested were passage 5, passage 7, and passage 9. (**Figure 3.3).**

Figure 3.2: Over subsequent passages the stromal cells showed morphological changes. Images represent sequential passages for the stromal cells. Passage 1 has more cells growing close together (A). Passage 2 has cells that look very similar to passage 1; they look healthy and proliferate well (B). Obvious cell morphology changes are seen in passage 8 (C). Cells lost structure and proliferative ability; this only worsens throughout the subsequent passages. Passage 14 has cells that have lost structure (D).

A

8/17/16   10/19/16   10/20/16   12/21/16

Count

P9
P7
P5
Isotype
Unstained

CD146 →

B

Count

P9
P7
P5
Unstained

OVA →

C

Count

P9
P7
P5
Isotype
Unstained

CD31 →

D

Count

P9
P7
P5
Isotype
Unstained

CD54 →

E

Count

P9
P7
P5
Isotype
Unstained

CD32 →

F

CD50

Legend: P9, P7, P5, Isotype, Unstained

G

MHC I

Legend: P9, P7, P5, Isotype, Unstained

H

MHC II

Legend: P9, P7, P5, Isotype, Unstained

I

CD80

Legend: P9, P7, P5, Isotype, Unstained

J

CD86

Legend: P9, P7, P5, Isotype, Unstained

K

L

Figure 3.3 Histograms showing positive and negative markers on Liver Sinusoidal Endothelial Cells. Representative histograms of positive markers include CD146 (**A**), scavenger receptor (OVA uptake (**B**), CD31 (**C**), CD54 (**D**), MHC I (**G**), MHC II (**H**), CD80 (**I**), and CD106 (**K**). Negative results, or very lowly expressed markers include CD32 (**E**), CD50 (**F**), CD86 (**J**), and CD206 (**L**). Each panel includes unstained, isotype control, passage 5 (red), passage 7 (cyan), and passage 9 (green) except from OVA (B). Isotype control not applicable for OVA uptake.

Three passage numbers were picked as different time points; early passage number, 5, a middle passage, 7, and a late passage number, 9. We tested these samples at different passage numbers to understand how stable the markers are and to what degree the markers are still present at later pasage numbers versus earlier passage numbers. Mean Fluorescence Intensity (MFI) was also calculated in order to have a more quantifiable parameter for the level of LSEC marker identification **(Figure 3.4).** We identified CD146, CD106, MHC I, MHC II, CD80, and CD54 as markers that were expressed. We included controls of an unstained sample in each experiment, and a single color control in order to have an individual stain for the marker, the comparison between many passages (5, 7, 9), and lastly an isotype control. The isotype control was included to serve as a negative control in comparison to our single stain for a postive control.

The expression level on the positive samples varied which added another layer of compexicity. CD146 was present in all samples but at a different level in each. This was true for OVA uptake as well.. CD54 expression was clear on populations in three of four samples but had vastly
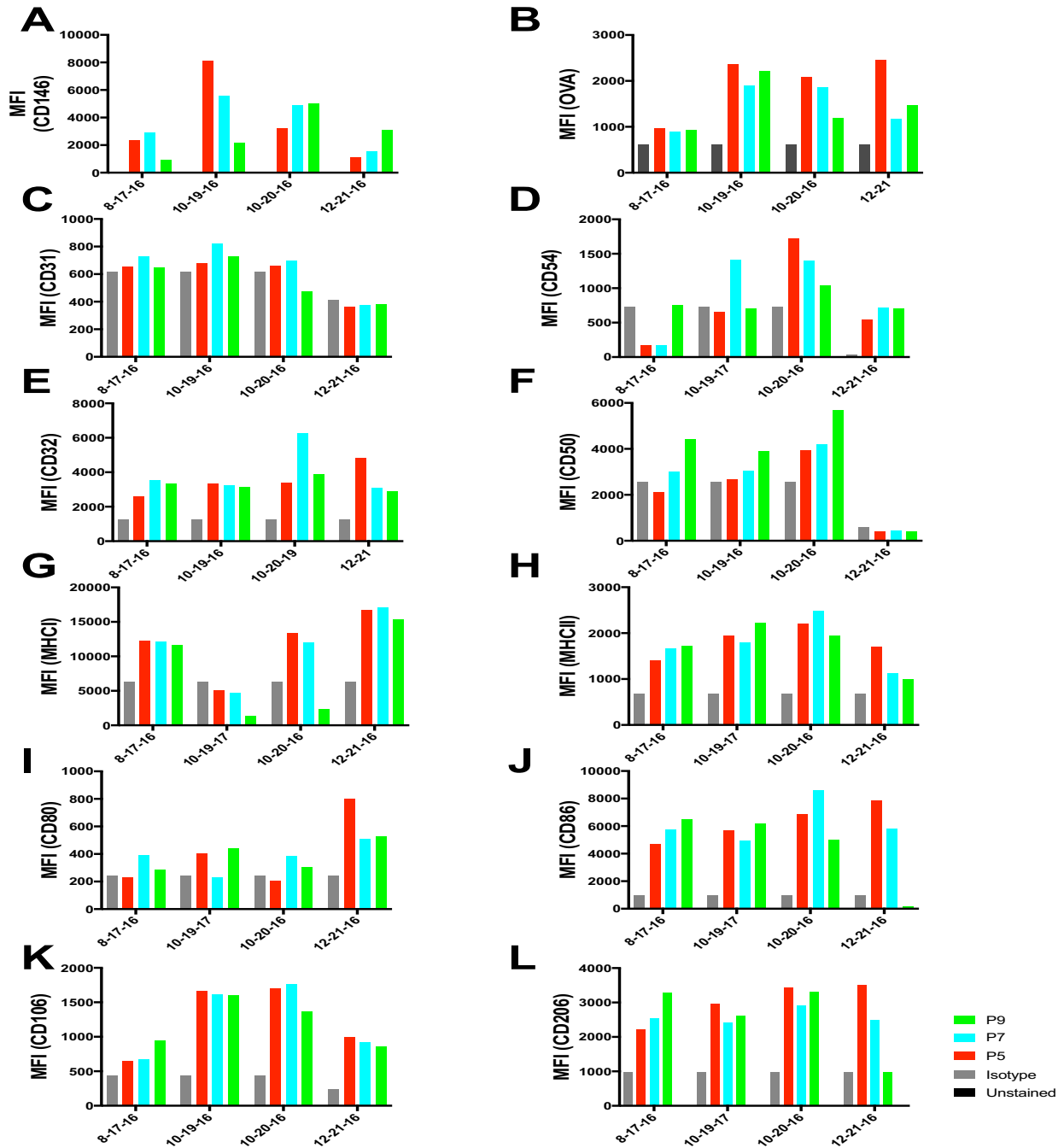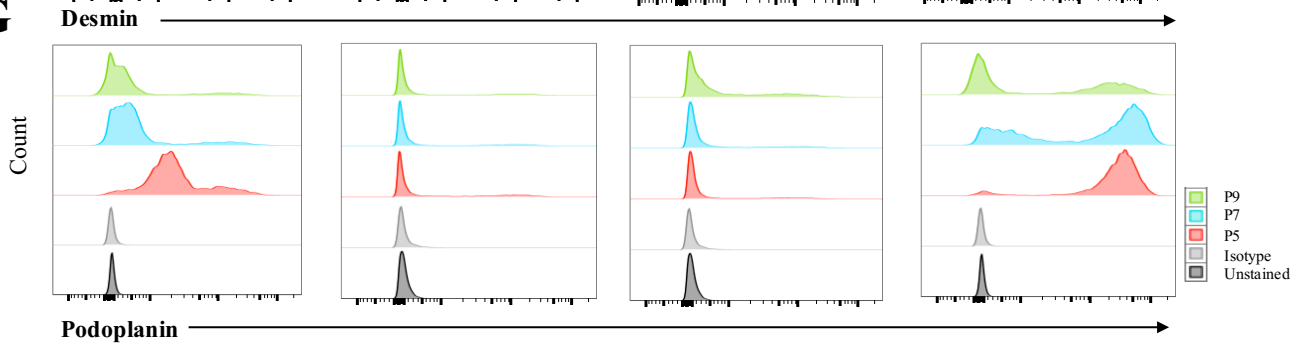

Figure 3.4 Mean Fluorescence Intensity (MFI) of markers on Liver Sinusoidal Endothelial Cells. The statistical data from figure 3.3 are represented and quantified here. Each marker and its respective MFI was quantified to show which marker is expressed and to what degree. All markers were tested with an isotype control (grey). Each bar graph includes unstained, isotype control, passage 5 (red), passage 7 (cyan), and passage 9 (green) except from OVA (B. Isotype control not applicable for OVA uptake; unstained included for OVA.

different flourscence intensities (**Figure 3.4, D).** These findings show the variability of the samples that were tested and illustrate the complexity of the project. CD32, CD50, CD86, and CD206 were not expressed on LSECs (**Figure 3.4, E, F, J, L).** These are seen as negative because of the lack of signal in the histograms in comparison to both the unstained control and the isotype control.

3.3 Identification of cellular markers for Hepatic Stellate Cell. The other stromal cellular subset that was explored, HSCs Mouse HSC had a set of markers that differentiated them from the LSECs. Mouse HSCs had Vitamin A, CD14, Vimentin, Desmin, GFAP and podoplanin. These cell markers were primarily intracellular markers (GFAP, Desmin, □-SMA, and Vimentin); however, certain surface markers were expressed including CD38, podoplanin, and CD14 s (Weiskirchen, 2014). Vitamin A is a defining characteristic for mouse liver stellate cells and is known to glow in UV light. Both the BV510 and FITC channel on the LSR II were both kept open to hopefully detect a positive signal in those channels which would indicate stellate cells due to the glowing of the Vitamin A in the UV light, however no signal was observed in any of our samples tested. The design was much the same as in the LSEC experiments. Each representative histogram contains the unstained control, isotype control, passage 5, passage 7, and passage 9 just as was shown previously (**Figure 3.5).** We found that Vimentin was expressed across passage numbers (**Figure 3.5).** Thus we found that what was known in about vimentin expression in HSCs in mice translated to human HSCs, (Uyama, 2006). Histograms are represented across different passages, 5, 7, and 9 just as in **figure 3.3**. These findings identify positive expression of Vimentin, □-SMA, CD14, and Podoplanin for HSCs and negative expression of GFAP, Desmin, and low expression of CD38.

A   8/17/16   10/19/16   10/20/16   12/21/16

CD14

B

Vimentin

C

Alpha-SMA

D

GFAP

**E**

CD38

23
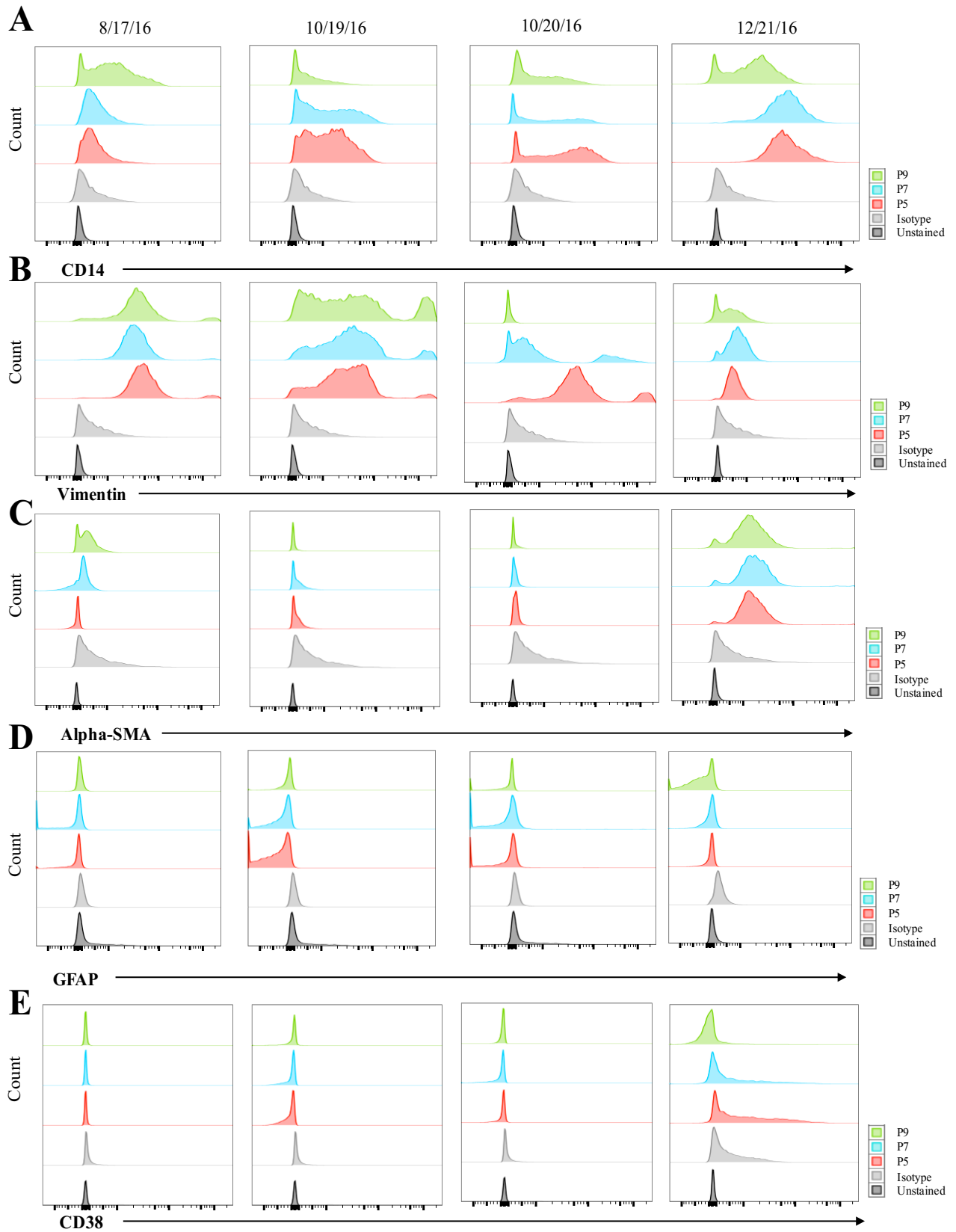
F
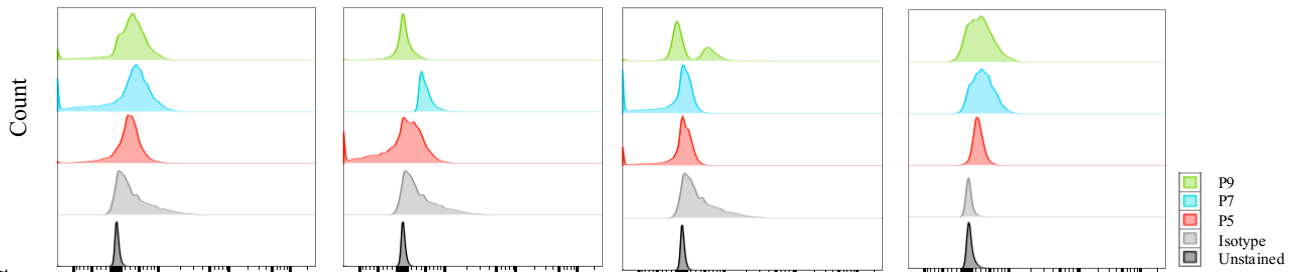
G

Figure 3.5 Hepatic Stellate Cells marker identification can be seen across different passage numbers. Representative histograms of the markers that were investigated for hepatic stellate cells. CD14 is seen as a positive marker (A) as is Vimentin (B) and only one sample for ▯-SMA (C, far right). Podoplanin (G) also has high levels of positive expression. Negative expression can be seen in GFAP (D) and three of four samples in CD38 (E).

MFI was also calculated to quantify the data that are represented in the histograms (**Figure 3.5**) (**Figure 3.6**).

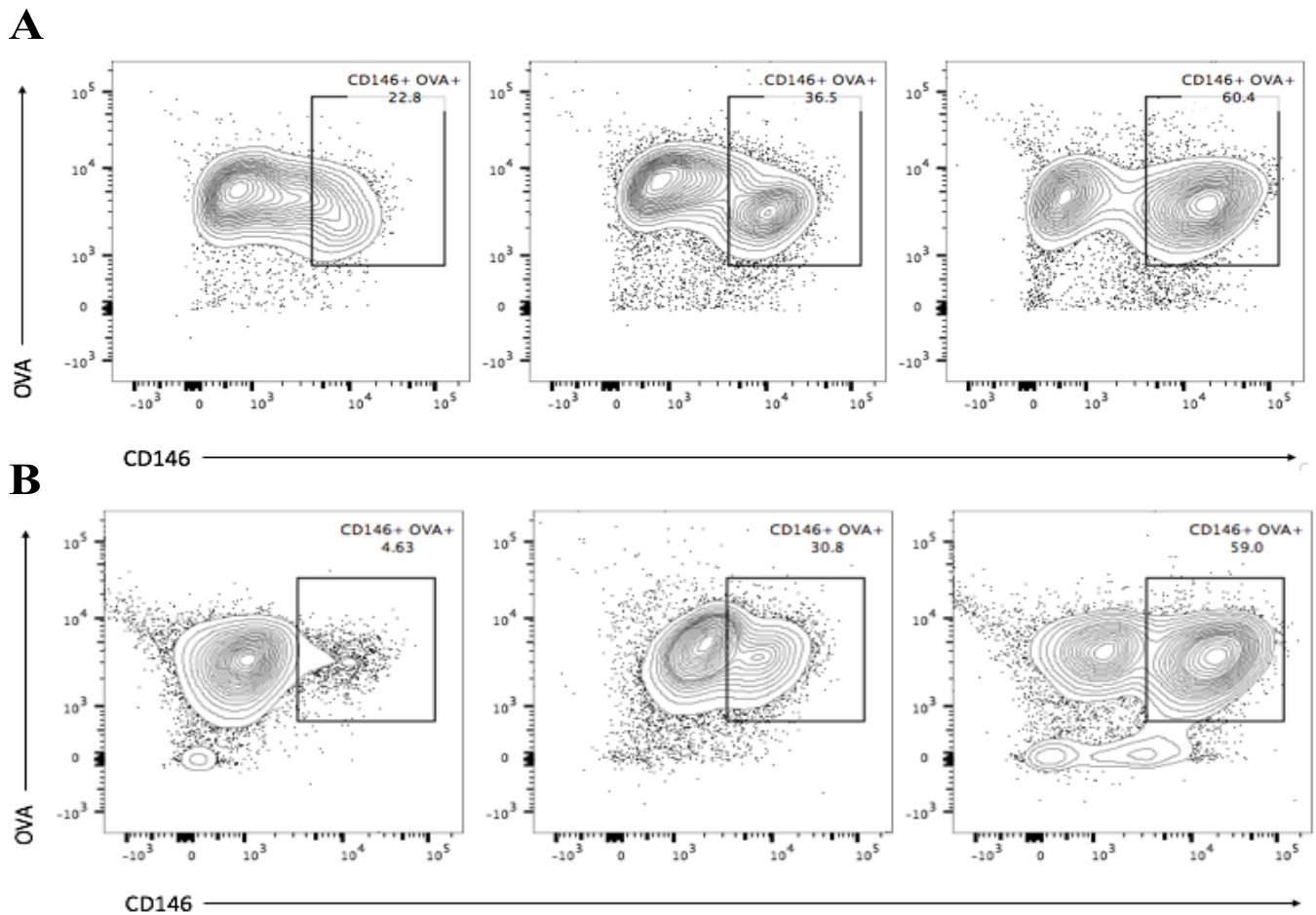**3.4 Population shift from single positive cells into double positive population shown with CD146+ and OVA+.** Interestingly, across different passages there was a strong population shift from single positive cells into double positive expression for both CD146 and OVA, two LSEC markers (**Figure 3.7**). This was seen in different human samples when comparing passage 5, 7, and 9. The two depictions show one sample from a patient who had not undergone chemotherapy treatment (**Figure 3.7, A**) and one sample from a patient who has undergone chemotherapy (**Figure 3.7, B**). Respective contour plots for each sample are shown across all three passages (**Figure 3.7**).
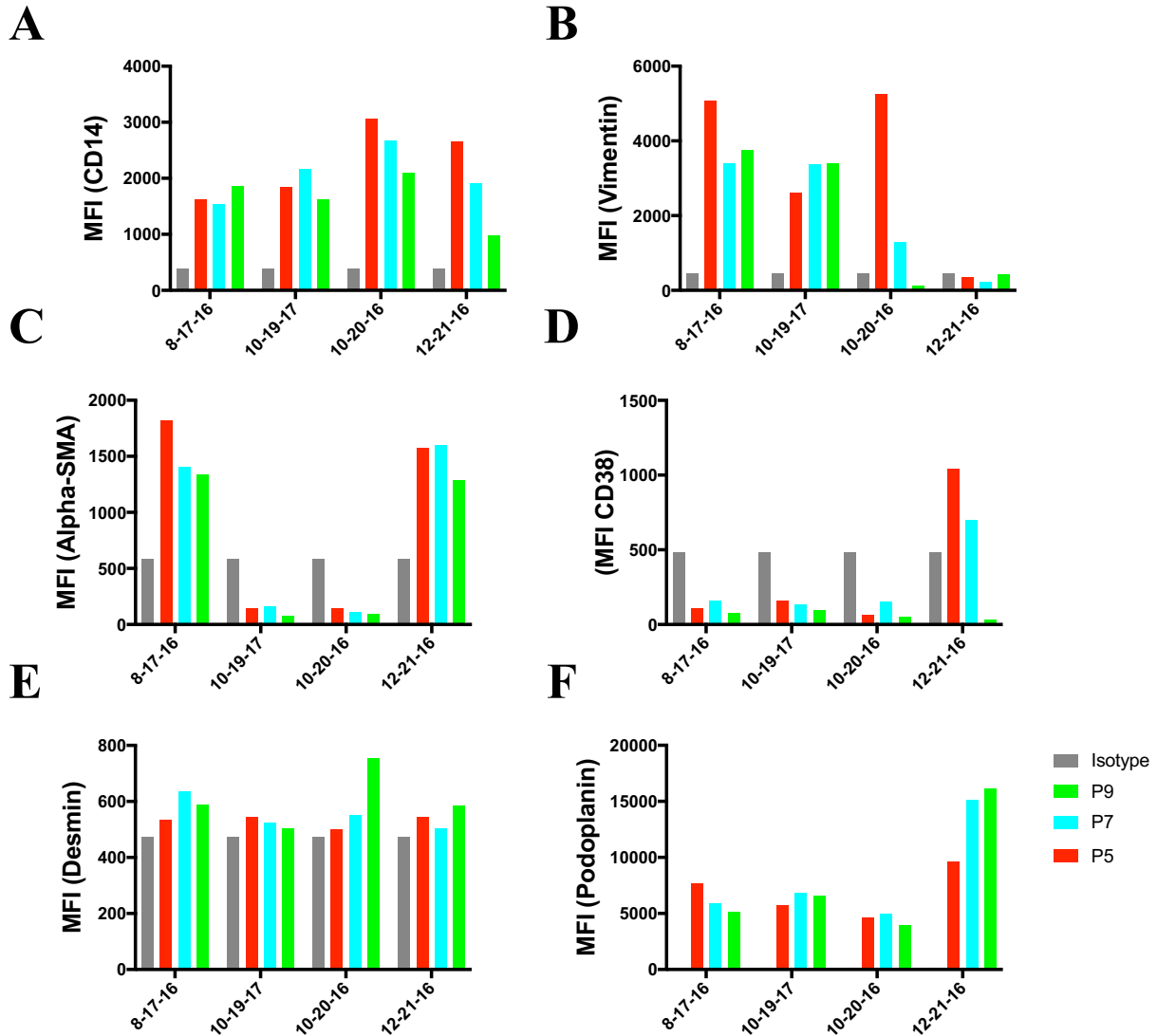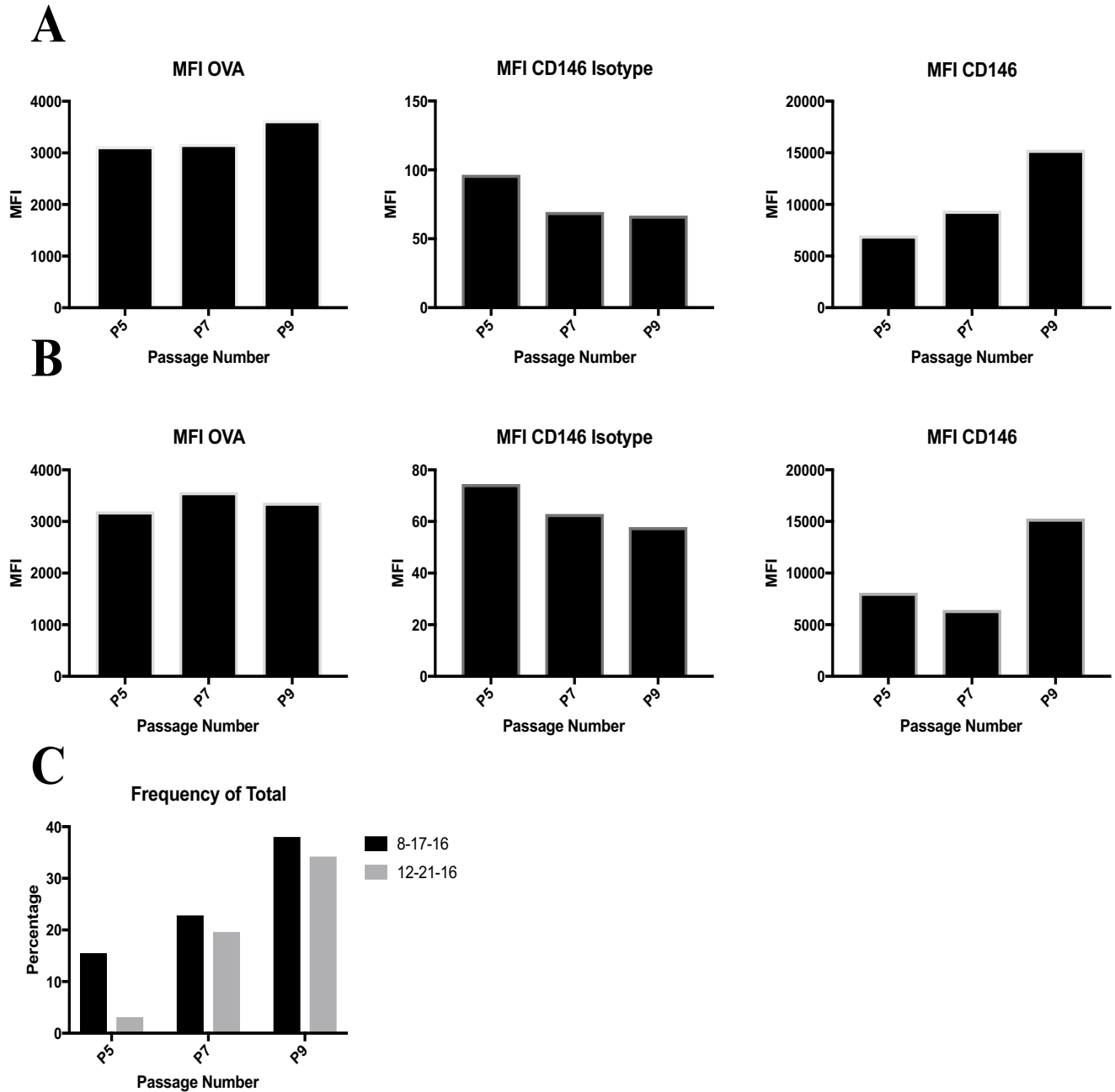
Figure 3.6 Mean Fluorescence Intensity (MFI) of Hepatic Stellate Cells. Statistical data of figure 3.5 are shown with the MFI data. MFI is quantified to show which marker is expressed and to what degree. All markers were tested with an unstained control and an isotype control (grey). Each bar graph includes isotype control, passage 5 (red), passage 7 (cyan), and passage 9 (green). Positive expression is seen in HSC activation marker CD14 (A), intracellular stain for Vimentin (B), and podoplanin (F). Negative expression is seen in CD38 (D), very low expression is seen in Desmin (E).

CD146 and OVA are two very strong markers for the murine LSEC population which is why we investigated both of them in human LSECs. The population shift becomes very interesting when looking at passage 5 for both samples which show a double positive population being less than 25% of the total cell count for both samples. In later passages the total population that is double

positive increases up to 60% by passage 9 (**Figure 3.7**). MFI for OVA, CD146, and isotype also were investigated. The MFI for OVA did not shift considerably over the three passages (**Figure 3.8 A and B**, **left**) for either sample: 8/17/16 (**Figure 3.8, A**) or 12/21/16 (**Figure 3.8, B**). However, CD146 expression changed considerably from passage 5 to passage 9 there was a dramatic increase across passages (**Figure 3.8 A and B, right).** Frequency of the double positive population changed over time, starting at less than 25% of the total population and becoming 60% of the total population (**Figure 3.8, C).**

A

B

Figure 3.7 Population shift in CD146+ OVA+ cells across passages. Representation of contour plots show dramatic shifts in cellular populations for CD146+ OVA+ cells across different passages that include passage 5, passage 7, and passage 9 for human liver sample digested on 8/17/16 (**A, left to right**). The cellular population shift between a low population of CD146+ OVA+ for passage 5 increases in different samples as well, this can be represented in human liver sample 12-21-16 (**B, left to right**). The shift in population can be seen in samples that have either not undergone chemotherapy treatment and those that have (**A and B).**

A

MFI OVA

MFI CD146 Isotype

MFI CD146

B

MFI OVA

MFI CD146 Isotype

MFI CD146

C

Frequency of Total

■ 8-17-16
■ 12-21-16

Figure 3.8: In order to fully understand how the population has shifted, MFI from figure 3.7 was calculated for each sample, for OVA, CD146 and CD146 expression compared to Isotype **(A and B).** 8/17/16 **(A)**. 12/21/16 **(B)**. While the OVA population didn't increase as dramatically as expected **(A and B left),** CD146 MFI increased drastically across passage numbers **(A and B, right).** The total number of cells that presented with this double positive population increased across passage numbers and is shown as a frequency of total bar graph **(C).**

Chapter 4: Discussion

In this thesis, we investigated two subsets of human liver stromal cells, Liver Sinusoidal Endothelial Cells and Hepatic Stellate Cells. This was done in a number of ways: we analyzed growth rate, and extracellular markers and intracellular markers for LSEC and HSC populations. These criteria were examined and tested across different passages of human liver samples *in vitro* to gain insight into the biology of human LSEC and HSC stromal cells. We addressed the following questions: 1) what are the different cellular markers on these cells, 2) how well are these markers expressed, and 3) do stromal cells maintain these cellular markers over the course of cellular expansion? We were able to compare markers for each of the two subsets in order to determine the differences between them at different passages and between the different samples acquired. This information provides a better understanding of the two cellular subsets and helps identify markers present on these human cells in culture. Previous work has been done mainly in mice. Cellular markers that were tested previously in mice include CD54, CD106, VAP, LSIGN, Mannose Receptors, Scavenger Receptors, CD80, CD86, CD40, CD4, CD11c (Knolle, 2001). We investigated whether markers expressed on mouse liver stromal cells were similarly expressed on human liver stromal cell populations.

Our studies show that human liver stromal cells are stable and can withstand many passages irrespective of patient diagnosis, age, sex, or therapy with chemotherapy or radiation. We had originally hypothesized that stromal cells derived from different diseases would have different growth patterns, but this was not the case. Our samples were from patients that did not have HIV, HPV, HCV, Hepatitis, Inflammatory Liver Disease, Non-Alcoholic Fatty Liver Disease, or other inflammatory liver diseases. Most samples were from patients with a diagnosis of cancer. A considerable number of our samples (7) were from patients treated with a chemotherapeutic drug

28

and we tracked which samples had been treated and which had not. Through these comparisons, we found no distinguishable difference between those from patients that had been through chemotherapeutic treatment and those that had not. Age and sex was another parameter that was explored but did not have any profound differences amongst the different samples.

In addition to sample variability and cellular growth rate, cellular markers were identified in the human samples that were expanded. The goal of these studies was to understand how stable the cellular markers, both intracellular and on the cell surface, are and if possibly the cells lose the markers during progressive passages. We found that specific cellular markers can be seen on stromal cells across many passages and also remain stable. The most prominent marker that was a positive identifier for LSECs was the surface marker CD146 which is expressed on epithelial cells. CD146 main function is maintenance of the integrity of the epithelial junctions which explains why it is seen on LSECs and not on HSC (Limmer, 2000). These LSECs were also CD45 negative which was to be expected as LSECs do not express CD45; this was used as a control to ensure there weren't any leukocytes in our population and give further proof that our sample had undergone purification and selection for stromal cells (Connolly, 2010). CD146+ signal was found in every sample tested regardless of passage number. This was a very important result because this was our first evidence that there was a clear marker that remained stable over many passages in human LSECs. However, there CD146 expression levels changed over the course of passaging and it is unclear why. For example, in sample 8-17-16 and 1-19-16 CD146 expression decreased over passages while in 10-20-16 and 12-21-16, CD146 expression increased across passages. These differences did not correlate with patient treatment history.

CD146 was not the only marker identified in human LSECs. Scavenger receptors are another highly selective feature of LSECs, specific to this cell type compared to HSCs. The ability

of the scavenger receptors on LSECs to uptake antigen is highly characteristic of LSECs because of their endocytic abilities, as demonstrated by the uptake of OVA in the treated sample. Similar to the changes in CD146 expression, there was a shift in uptake of OVA in the cell lines that was not consistent across samples. It was incredibly important to include CD146 and OVA in every experiment in order to have an LSEC identifier and exclude other cell types including leukocytes.

Worth noting, CD106 expression on LSECs has been questioned in the field where some studies claim LSECs do not express CD106 (Elvevold, 2007), while others claim there is expression (Karrar, 2007). We found some CD106 expression on human LSECs. Our histograms showed CD106 expression over time and MFI score and a positive signal amongst our samples, CD146 and scavenger receptors are not the only positive results seen; CD54, MHC I, CD32, CD80 were also expressed, as shown both in histograms and MFI score. Not all markers tested were positive expression though. We also investigated CD31, CD206, and CD50 (ICAM-3) but these showed either very low expression or, a negative signal.

CD45 was used for leukocyte exclusion in these experiments. After many experiments where CD45 was not detected, CD45 was later taken out of later experiments in order to open up the UV laser for the HSC experiments. This was important because it allowed for a dump channel (channel that could detect fluorescence without antibody) to be created in the violet laser in order to test fluorescence of vitamin A by the HSCs. Vitamin A glows excessively in the UV channel and is seen in the violet laser and is a positive identifier of HSCs (Kubota, 2007). We unfortunately, did not get signal for vitamin A in our studies. This could be due to many different things; we speculated that the cells may lose the capacity to maintain vitamin A storage in culture over many passages because we did not supplement Vitamin A in the media and the vitamin A simply became depleted. Based on studies of mouse HSCs we tested whether human HSCs expressed Vimentin,

osteopontin, ▯-SMA, and Desmin (Chagraoui, 2003). Other markers of interest were CD14 which is expressed on activated stellate cells, CD38, GFAP and podoplanin. It is known that ▯-SMA is a highly reliable marker for HSCs because it is absent from other liver resident cells. Interestingly, if HSCs are activated, ▯-SMA expression is increased which will lead to an increase in fibrosis in the environment (Morini, 2005). The expression of ▯-SMA is not only specific for identification of HSC but also important in understating the progression of fibrosis. GFAP is another characteristic marker of HSC that is typically quiescent in cells; if the cells lose expression of GFAP they become activated which starts the process of collagen production thus leading to fibrosis. We did not find any level GFAP expression, but we did find positive expression for ▯-SMA in two of the samples that steadily decreased across passage numbers. In regards to ▯-SMA, the two samples that were positive, both were very different; one sample was a patient treated with chemotherapy and one not. There isn't clear understanding why some were positive and others were not; it may be that over the course of many passages the cells start to lose expression or that simply that each sample is very different. Low levels of Desmin were seen in each and this was less than we had anticipated. However, high expression levels of CD14, Vimentin, and Podoplanin were quantified in all HSCs samples when comparing both the MFI values and the representative histograms. Further work with stimulation assays such as cytokine production, stimulation with LPS, and co-culture experiments is necessary to understand how expression of these markers may change over the course of multiple passage numbers.

The findings in this thesis show the variability of the stromal cell subsets and their durability over time. We have identified specific cellular markers to use in future studies of LSECs and HSCs. These markers will be useful for many applications such as cellular sorting of primary human tissue samples, transcriptional profiling using single cell RNA sequencing, purification of

LSEC or HSC for co-stimulatory assays, cytokine production assays, and many other biological

assays. The work provided in this thesis lays the groundwork for future studies of Liver Sinusoidal

Endothelial Cells and Hepatic Stellate Cells.

Chapter 5: Limitations and Perspectives

Our data have provided a quantifiable understanding of stromal cell growth rate. While we have found an average amount of time for the cells to reach confluence across different passages, it cannot be definitively stated how long it will take for each cell line to grow and it cannot be normalized for each subsequent sample that may be acquired. These cells are different for each sample which makes sense because of the different patient diagnoses. It is valuable to have an understanding of how long it will take from stage zero until passage 5 for example, because these cells do grow relatively slowly up until the first passage. Another variability in growth is that some cell lines had to go through a second digestion, or some needed to be left in the digestion mixture longer than others due to the toughness of the sample; these differences affect how quickly the cells grow. While it was not a normal procedure for the samples to go through a second digestion, it was not uncommon for large samples to undergo a second digestion due to size of the sample. The larger samples needed a second digestion.

Sample variables involving time impacted our studies. We tried our absolute best to acquire and digest the sample as soon as possible in order to limit the amount of time the whole tissue sat either on the bench top post-surgical resection, in the refrigerator, on ice, etc. for fear of having cells die. We tried to be conscientious about the whole process in order to have our samples be the healthiest possible and keep the cells in their best possible condition in the hopes that this would lead to healthy growth in culture.

While our results point to what markers are stable, a major limiting factor was the passage at which cells could be tested. We did not want to use all of our earliest passage number samples for marker studies, because when those passages are depleted, we cannot get them back. We anticipate that the earliest passage numbers, (P0 and P1) may present with different expression of

markers but we did not use those cells for fear of depleting our entire sample. Expansion of frozen cells was carefully calculated as to which passage number could be used when thawing cells for different liver samples. The earliest passage number that we could freeze was passage 3, but not every cell line grew enough to be able to freeze cells at this specific cell passage; others started to be frozen at passage 4. Growth and confluence of the cells was a deciding factor in how to move forward with experiments.

Our experiments give us insight into which markers are able to withstand trypsin and many cellular passage numbers but that do not answer all of our questions. A remaining question is at what passage number do the markers start to lose expression? Some experiments were done at passage number 12 and tested against other early passage numbers which showed positive signal but also quite a bit more background noise which could have been due to more broken, dead or dying cells in the media. The longest cultured cells became very sticky and were difficult to pellet and resuspended.

While there were definitely areas of the project that proved challenging, future studies are extremely exciting. The identification of marker that are present on these stromal cells will allow us to do many future experiments including the use of single cell RNA sequencing to perform transcriptional profiling. Understanding when human samples in culture lose vitamin A storage would be beneficial as well because this could provide another means to sort out cells. We by no means explored a comprehensive list of markers; there are other that could be investigated and tested *in vitro.* By having specific markers such as CD146 for LSECs and ⎕-SMA for HSCs, cellular sorting of these defined populations will be possible. When purified samples are then acquired using these markers many other assays may be done to understand the functions of these cells including stimulation of the cells and co-culture experiments.

Concluding statements:

In this thesis we sought to understand human liver stromal cells in different capacities including LSEC marker identification, HSC marker identification, and cellular growth rate. Our aim was to understand what changes occur in cellular expression of markers and cellular growth rate. Experiments revealed markers that are positive for LSECs such as CD146, scavenger receptors, and CD106; whereas positive expression on HSCs was also seen with Vimentin, □-SMA, and Podoplanin. Identification of markers that are negative such as CD50, MHC II for LSECs, and GFAP for HSC proved to be just as valuable in that negative markers have given us an understanding of what not to use as a selective marker for these cells. While it was known in mice that Vitamin A glows when excited by the UV laser, we did not find this to be true in our experiments with human stromal cells. In addition to testing cellular markers, we polished an established protocol to maintain human stromal cells in culture for over 14 passages which then gave us insight into how these samples grow. By understanding the growth capacities of these cells we were able to optimize the amount of cells acquired. This project helped us learn about human LSECs and HSCs by using published knowledge from mice and translating that work into studies with human samples. Our results provide a foundation for future studies with human liver stromal cells.

References:

1. American Liver Foundation. *Liver Disease: The Big Picture*. Oct. 18, 2013. http://www.liverfoundation.org/education/liverlowdown/ll1013/bigpicture/

2. Arimoto, J., Ikura, Y., Suekane, T. et al. Expression of LYVE-1 in sinusoidal endothelium is reduced in chronically inflamed human livers. J Gastroenterology. (2010) 45: 317. doi:10.1007/s00535-009-0152-5

3. Bertolino P, Bowen DG, McCaughan GW, Fazekas de St Groth B (2001) Antigen-specific primary activation of CD8+ T cells within the liver. J Immunol 166(9):5430–5438

4. Braet F, Wisse E. Structural and functional aspects of liver sinusoidal endothelial cell fenestrae: a review. *Comparative Hepatology*. 2002; 1:1. doi:10.1186/1476-5926-1-1

5. Chagraoui, J., Lepage-Noll, A., Anjo, A., Uzan, G., Charbord, P. Fetal liver stroma consists of cells in epithelial-to-mesenchymal transition Blood Apr 2003, 101 (8) 2973-2982; DOI: 10.1182/blood-2002-05-1341

6. Chen W, Rock JB, Yearsley MM, Ferrell LD, Frankel WL. Different collagen types show distinct rates of increase from early to late stages of hepatitis C-related liver fibrosis. Hum Pathol 2014;45: 160–165. doi: 10.1016/j.humpath.2013.08.015. pmid:24321525

7. Cheng F, Shen Y, Mohanasundaram P, et al. Vimentin coordinates fibroblast proliferation and keratinocyte differentiation in wound healing via TGF-β–Slug signaling. *Proceedings of the National Academy of Sciences of the United States of America*. 2016;113(30): E4320-E4327. doi:10.1073/pnas.1519197113.

8. Connolly, MK., et al. In Hepatic Fibrosis, Liver Sinusoidal Endothelial Cells Acquire Enhanced Immunogenicity. The Journal of Immunology August 15, 2010, 185 (4) 2200-2208; DOI: 10.4049/jimmunol.1000332

9. Copland IB. Mesenchymal stromal cells for cardiovascular disease. *Journal of Cardiovascular Disease Research*. 2011;2(1):3-13. doi:10.4103/0975-3583.78581.

10. Dave JM, Bayless KJ. Vimentin as an integral regulator of cell adhesion and endothelial sprouting. Microcirculation 21: 333–344, 2014.

11. De Leeuw A.M., Brouwer A., Knook D.L. Sinusoidal endothelial cells of the liver: Fine structure and function in relation to age. J. Electron. Microsc. Tech. 1990; 14:218–236. doi: 10.1002/jemt.1060140304.

12. DeLeve LD. Liver Sinusoidal Endothelial Cells in Hepatic Fibrosis. *Hepatology (Baltimore, Md)*. 2015;61(5):1740-1746. doi:10.1002/hep.27376.

13. DeLeve LD. Liver sinusoidal endothelial cells and liver regeneration. *The Journal of Clinical Investigation*. 2013;123(5):1861-1866. doi:10.1172/JCI66025.

14. Elvevold, K., Smedsrød, B., Martinez I. American Journal of Physiology-Gastrointestinal and Liver Physiology. Feb 2008, 294 (2) G391 G400; DOI: 10.1152/ajpgi.00167.2007

15. Friedman SL. Hepatic Stellate Cells: Protean, Multifunctional, and Enigmatic Cells of the Liver. *Physiological reviews*. 2008;88(1):125-172. doi:10.1152/physrev.00013.2007.

16. Friedman SL, ed. *The Hepatic Stellate cell.* Vol. 21. New York: Thieme; 2001.

17. Fomin ME, Zhou Y, Beyer AI, Publicover J, Baron JL, Muench MO. Production of Factor VIII by Human Liver Sinusoidal Endothelial Cells Transplanted in Immunodeficient uPA Mice. 2013. PLoS ONE 8(10): e77255. doi:10.1371/journal.pone.0077255

18. Haldar, D., et al. Mesenchymal stromal cells and liver fibrosis: a complicated relationship. FASEB J. December 2016. 30:3905-3928; doi: 10.1096/fj.201600433R

19. Höchst B, Schildberg FA, Sauerborn P, Gäbel YA, Gevensleben H, Goltz D *et al*. Activated human hepatic stellate cells induce myeloid derived suppressor cells from peripheral blood monocytes in a CD44-dependent fashion. *J Hepatol* 2013; 59: 528–535

20. Höchst, B., Schildberg, F. A., Böttcher, J., Metzger, C., Huss, S., Türler, A., Overhaus, M., Knoblich, A., Schneider, B., Pantelis, D., Kurts, C., Kalff, J. C., Knolle, P. and Diehl, L. (2012), Liver sinusoidal endothelial cells contribute to CD8 T cell tolerance toward circulating carcinoembryonic antigen in mice. Hepatology, 56: 1924–1933. doi:10.1002/hep.25844

21. Hu, J., Hu, S., Ma, Q., Wang, X., Zhou, Z., Zhang, W. ... Xu, W. Immortalized mouse fetal liver stromal cells support growth and maintenance of human embryonic stem cells. 2012. Oncology Reports, 28, 1385-1391. http://dx.doi.org/10.3892/or.2012.1909

22. Janeway CA Jr, Travers P, Walport M, et al. *The major histocompatibility complex and its functions.* Immunobiology: The Immune System in Health and Disease. 5th edition. New York: Garland Science; 2001.

23. Ju, C., Tacke, F. Hepatic macrophages in homeostasis and liver diseases: from pathogenesis to novel therapeutic strategies. *Cell Mol Immunol*. 2016;13:316–327.

24. Karrar A, Broomé U, Uzunel M, Qureshi AR, Sumitran-Holgersson S. Human liver sinusoidal endothelial cells induce apoptosis in activated T cells: a role in tolerance induction. *Gut*. 2007;56(2):243-252. doi:10.1136/gut.2006.093906.

25. Kawai Y, Smedsrod B, Elvevold K, Wake K. *Uptake of lithium carmine by sinusoidal endothelial and Kupffer cells of the rat liver: new insights into the classical vital staining and the reticulo-endothelial system. Cell Tissue Res* 292*: 395–410,*1998

26. Kratzer, A., Chu, H. W., Salys, J., Moumen, Z., Leberl, M., Bowler, R., Cool, C., Zamora, M. and Taraseviciene-Stewart, L. (2013), Endothelial cell adhesion molecule CD146: implications for its role in the pathogenesis of COPD. J. Pathol., 230: 388–398. doi:10.1002/path.4197

27. Knolle PA, Wohlleber D. Immunological functions of liver sinusoidal endothelial cells. *Cellular and Molecular Immunology*. 2016;13(3):347-353. doi:10.1038/cmi.2016.5.

28. Knolle, PA. Staying local – antigen presentation in the liver. Curr. Opin. Immunol., 40 (2016), pp. 36–42

29. Knolle, P.A., Böttcher, J. & Huang, LR. Med Microbiol Immunol (2015) 204: 21. doi:10.1007/s00430-014-0371-0

30. Limmer, A., et al., 2000. Efficient presentation of exogenous antigen by liver endothelial cells to CD8^{+} T cells results in antigen-specific T-cell tolerance. Nat. Med. 6: 1348–1354.

31. Loo CKC, Pereira TN, Pozniak KN, Ramsing M, Vogel I, Ramm GA. The development of hepatic stellate cells in normal and abnormal human fetuses – an immunohistochemical study. *Physiological Reports*. 2015;3(8):e12504. doi:10.14814/phy2.12504.

32. MacPhee PJ, Schmidt EE, Groom AC (1995) Intermittence of blood flow in liver sinusoids, studied by high-resolution in vivo microscopy. Am J Physiol 32:G692–G698

33. March, S., et al. *Identification and Functional Characterization of the Hepatic Stellate Cell CD38 Cell Surface Molecule*. The American Journal of Pathology, V170, 1, 176-187.

34. Meyer J, Gonelle-Gispert C, Morel P, Bühler L (2016) Methods for Isolation and Purification of Murine Liver Sinusoidal Endothelial Cells: A Systematic Review. PLoS ONE 11(3): e0151945. doi:10.1371/journal.pone.0151945

35. Morini, S., et al. GFAP expression in the liver as an early marker of stellate cells activation. Italian Journal of Anatomy and Embryology. Oct 2005. 110(4): 193-207.

36. Pradere, J.-P., et al. Hepatic macrophages but not dendritic cells contribute to liver fibrosis by promoting the survival of activated hepatic stellate cells in mice. Hepatology 58,1461–1473

37. Ramachandran, P., Iredale, J. P. (2012) Liver fibrosis: a bidirectional model of fibrogenesis and resolution. QJM 105, 813–817

38. Rifaat Safadi R, Friedman SL. Hepatic Fibrosis -- Role of Hepatic Stellate Cell Activation. MedGenMed, 4(3), 2002 [formerly published in Medscape Gastroenterology eJournal 4(4), 2002].

39. Ringden, O. Mesenchymal stromal cells as treatment for chronic GVHD. *Bone Marrow Transplantation*. Nature. *Bone Marrow Transplantation* (2011) 46**,** 163–164; doi:10.1038/bmt.2010.27

40. Rockey DC. Hepatic blood flow regulation by stellate cells in normal and injured liver. Semin Liver Dis. 2001;21:337-350.

41. Rojkind, Marcos et al. Collagen Types in Normal and Cirrhotic Liver. Gastroenterology, V.76.4, 710-719

42. Rojewski MT, Weber BM, Schrezenmeier H. Phenotypic Characterization of Mesenchymal Stem Cells from Various Tissues. *Transfusion Medicine and Hemotherapy*. 2008;35(3):168-184. doi:10.1159/000129013.

43. Schildberg FA., et al., 2008. Liver sinusoidal endothelial cells veto CD8 T cell activation by antigen-presenting dendritic cells. Eur. J. Immunol. 38:957–967.

44. Schildberg et al., 2015. Schildberg F.A., Sharpe A.H., and Turley S.J.: Hepatic immune regulation by stromal cells. Curr. Opin. Immunol. 2015; 32c: pp. 1-6

45. Schildberg, F. A., Wojtalla, A., Siegmund, S. V., Endl, E., Diehl, L., Abdullah, Z., Kurts, C. and Knolle, P. A. (2011), Murine hepatic stellate cells veto CD8 T cell activation by a CD54-dependent mechanism. Hepatology, 54: 262–272. doi:10.1002/hep.24352

46. Schildberg FA, Hegenbarth SI, Schumak B, Scholz K, Limmer A, Knolle PA. Liver sinusoidal endothelial cells veto CD8 T cell activation by antigen-presenting dendritic cells. *Eur J Immunol* 2008

47. Schildberg FA, Wojtalla A, Siegmund SV, Endl E, Diehl L, Abdullah Z *et al*. Murine hepatic stellate cells veto CD8 T cell activation by a CD54-dependent mechanism. *Hepatology* 2011; 54: 262–272.

48. Schildberg, FA *et al.* Improved transplantation outcome by epigenetic changes. Transpl. Immunol., 23 (2010), pp. 104–110

49. Schurich, A., Böttcher, J. P., Burgdorf, S., Penzler, P., Hegenbarth, S., Kern, M., Dolf, A., Endl, E., Schultze, J., Wiertz, E., Stabenow, D., Kurts, C. and Knolle, P. (2009), Distinct kinetics and dynamics of cross-presentation in liver sinusoidal endothelial cells compared to dendritic cells. Hepatology, 50: 909–919. doi:10.1002/hep.23075

50. Schrage A, Loddenkemper C, Erben U, et al. Murine CD146 is widely expressed on endothelial cells and is recognized by the monoclonal antibody ME-9F1. *Histochemistry and Cell Biology*. 2008;129(4):441-451. doi:10.1007/s00418-008-0379-x.

51. Scholzel K, Schildberg FA, Welz M, Borner C, Geiger S, Kurts C *et al*. Transfer of MHC-class-I molecules among liver sinusoidal cells facilitates hepatic immune surveillance. *J Hepatol* 2014; 61: 600–608.

52. Stenger, E, et. al., Bone Marrow Derived Mesnechymal Stromal Cclls from Patients with Sickle Cell Disease Display Intact Functionality. *Biology of Blood and Marrow Transplantation.* January 26, 2017. dx.doi.org.ezp-prod1.hul.harvard.edu/10.1016/j.bbmt.2017.01.081

53. Thomson, AW., Knolle, PA. Antigen-presenting cell function in the tolerogenic liver environment. *Nature Reviews Immunology* 10, 753-766 (November 2010). doi:10.1038/nri2858

54. Turley, SJ., Cremasco, V., Astarita, JL. Immunological hallmarks of stromal cells in the tumour microenvironment. *Nature Reviews Immunology* 15, 669–682 (2015) doi:10.1038/nri3902

55. Uyama N, Zhao L, Van Rossen E, et al. Hepatic stellate cells express synemin, a protein bridging intermediate filaments to focal adhesions. *Gut*. 2006;55(9):1276-1289. doi:10.1136/gut.2005.078865.

56. Wohlleber D., Knolle, PA. The role of liver sinusoidal cells in local hepatic immune surveillance. *Clinical & Translational Immunology* (2016) 5, e117; doi:10.1038/cti.2016.74

57. Xu, F., et al., LSECtin expressed on melanoma cells promotes tumor progression by inhibiting antitumor T-cell responses. *Cancer Research* (2014). Doi: 10.1158/0008-5472.CAN-13-2690

Appendix:

Date Collected	Patient data	Description of tissue	Visual
8/16/16	Sex:Male Age: 60 **Diagnosis:** Gallbladder cancer	Tissue was approximately 3 cm in size, soft	N/A
9/12/16**	Sex: Female Age: 72 **Diagnosis:** Intrahepatic choloangiocarcinoma	Tissue was small in size, approx.. 2 cm; digested quickly, soft tissue	N/A
9/27/16	Sex: Female Age: 72 **Diagnosis:** choloangiocarcinoma	Tissue was approx. 3 com in size, digested quickly	N/A
10/7/16*	Sex: Female Age: 82 **Diagnosis:** intrahepatic choloangiocarcinoma	Small sample, approx. 2 cm, white spots on liver, soft tissue	
10/19/16*	Sex: Female Age: 80 **Diagnosis:** gallbladder carcinoma	Small sample, approx. 2 cm; large white spots on sample, tougher tissue, didn't want to go through mashing step easily	
10/20/16	Sex: Female Age: 77 **Diagnosis:** Metastatic colorectal cancer	Much larger sample, tough tissue, very difficult to cut up, didn't want to mash either	
10/24/16	Sex: Female Age: 61 **Diagnosis:** intrahepatic choloangiocarcinoma	Large sample, much softer than 10/20, easy to digest, mashed well no apparent white spots	
10/31/16*	Sex: Male Age: 72 **Diagnosis:** colon carcinoma with liver metastasis	Very large, dense sample. Large white patches throughout, tough to cut through, didn't want to digest	

11/3/16	**Sex:** Male	Very small sample, easy to digest.	
	Age: 67		
	Diagnosis: metastatic colorectal cancer		
11/8/16	**Sex:** Female	Small sample, large white patches/holes in the sample, cut easy, digested well	
	Age: 55		
	Diagnosis: biliary cystadenoma of the left liver		
12/20/16*	**Sex:** Female	Smaller sample size, easy to digest	
	Age: 48		
	Diagnosis: lung cancer liver metastasis		
12/21*	**Sex:** Female	Small sample size, easy to digest	
	Age: 61		
	Diagnosis: Metastatic colorectal cancer		
1/5*	**Sex:** Male	Very small sample, no apparent white spots, digested quickly	
	Age: 71		
	Diagnosis: Colon carcinoma		
1/6	**Sex:** Female	Larger sample, digested well, very soft tissue	
	Age: 65		
	Diagnosis: hilar cholangiocarcinoma		
1/20	**Sex:** Female	Small sample, digested easily, very soft tissue, easy to cut through and mash	
	Age: 38		
	Diagnosis: biliary colic and biliary cysts		
1/25	**Sex:** Male	Very large/dense sample, difficult to cut, very difficult to mash. Sample did not want to digest.	
	Age: 48		
	Diagnosis: metastatic renal cell carcinoma		

2/1	Sex: Female	Very small sample with strange formation on one side of the sample. No apparent white spots, digested very quickly	
	Age: 45		
	Diagnosis: 5cm hepatic adenoma		
2/2	Sex: Male	Large sample, very fatty tissue, tough to digest because of all of the fat tissue, no apparent white spots	
	Age: 43		
	Diagnosis: large left hepatic mass		

Table 1.3 Human tissue sample data and observation allow for characterization of disease and origin of sample. The quantification of data that is acquired from these samples allows for experimental design to be shifted based on populations that would be selected for; i.e. male vs female experiments, similar diagnosis, chemotherapy treatment and other options. *patient underwent chemotherapy **patient underwent radiation treatment